Iriko H, Jin L, Kaneko O, Takeo S, Han ET, Tachibana M, Otsuki H, Torii M, Tsuboi T	A small-scale systematic analysis of alternative splicing in *Plasmodium falciparum*	**Parasitol Int.**	58	196-199	2009
Otsuki H, Kaneko O, Thongkukiatkul A, Tachibana M, Iriko H, Takeo S, Tsuboi T, Torii M	Single amino acid substitution in *Plasmodium yoelii* erythrocyte ligand determines its localization and controls parasite virulence	**Proc Natl Acad Sci U S A.**	106	7167-7172	2009
Takeo S, Arumugam TU, Torii M, Tsuboi T.	Wheat germ cell-free technology for accelerating the malaria vaccine research	**Expert Opin Drug Discov.**	4	1191-1199	2009
Arakawa T, Tachibana M, Miyata T, Harakuni T, Kohama H, Matsumoto Y, Tsuji N, Hisaeda H, Stowers A, Torii M, Tsuboi T	Malaria ookinete surface protein-based vaccination via the intranasal route completely blocks parasite transmission in both passive and active vaccination regimens in a rodent model of malaria infection	**Infect Immun,**	77	5496–5500	2009

研究成果の刊行物・別刷

Parasitology International 58 (2009) 29–35

Contents lists available at ScienceDirect

Parasitology International

journal homepage: www.elsevier.com/locate/parint

Rhoptry neck protein RON2 forms a complex with microneme protein AMA1 in *Plasmodium falciparum* merozoites☆

Jun Cao [a,b], Osamu Kaneko [a,c,*], Amporn Thongkukiatkul [d], Mayumi Tachibana [a], Hitoshi Otsuki [a], Qi Gao [b], Takafumi Tsuboi [e,f], Motomi Torii [a]

[a] Department of Molecular Parasitology, Ehime University Graduate School of Medicine, Shitsukawa, Toon, Ehime 791-0295, Japan
[b] Malaria Department, Jiangsu Institute of Parasitic Diseases, Meiyuan, Wuxi, Jiangsu 214064, People's Republic of China
[c] Department of Protozoology, Institute of Tropical Medicine (NEKKEN), Nagasaki University, Sakamoto, Nagasaki 852-8523, Japan
[d] Department of Biology, Faculty of Science, Burapha University, Chonburi 20131, Thailand
[e] Cell-Free Science and Technology Research Center, Ehime University, Matsuyama, Ehime 790-8577, Japan
[f] Venture Business Laboratory, Ehime University, Matsuyama, Ehime 790-8577, Japan

ARTICLE INFO

Article history:
Received 12 August 2008
Received in revised form 15 September 2008
Accepted 18 September 2008
Available online 7 October 2008

Keywords:
AMA1
Erythrocyte invasion
Merozoite
Plasmodium falciparum
Rhoptry

ABSTRACT

Erythrocyte invasion is an essential step in the establishment of host infection by malaria parasites, and is a major target of intervention strategies that attempt to control the disease. Recent proteome analysis of the closely-related apicomplexan parasite, *Toxoplasma gondii*, revealed a panel of novel proteins (RONs) located at the neck portion of the rhoptries. Three of these proteins, RON2, RON4, and RON5 have been shown to form a complex with the microneme protein Apical Membrane Protein 1 (AMA1). This complex, termed the Moving Junction complex, localizes at the interface of the parasite and the host cell during the invasion process. Here we characterized a RON2 ortholog in *Plasmodium falciparum*. *Pf*RON2 transcription peaked at the mature schizont stage and was expressed at the neck portion of the rhoptry in the merozoite. Co-immunoprecipitation of *Pf*RON2, *Pf*RON4 and *Pf*AMA1 indicated that the complex formation is conserved between *T. gondii* and *P. falciparum*, suggesting that co-operative function of the rhoptry and microneme proteins is a common mechanism in apicomplexan parasites during host cell invasion. *Pf*RON2 possesses a region displaying homology with the rhoptry body protein *Pf*RhopH1/Clag, a component of the RhopH complex. However, here we present co-immunoprecipitation studies which suggest that *Pf*RON2 is not a component of the RhopH complex and has an independent role. Nucleotide polymorphism analysis suggested that *Pf*RON2 was under diversifying selective pressure. This evidence suggests that RON2 appears to have a fundamental role in host cell invasion by apicomplexan parasites, and is a potential target for malaria intervention strategies.

1. Introduction

Malaria is one of the most prevalent and deadly global infectious diseases, more than half of the world's population is at the risk of infection, and over 300 million people develop clinical disease each year of which 2 million are fatal [1]. Clinical malaria results from the replication of protozoan parasites of the genus *Plasmodium* in the circulating erythrocytes of the host. During the time between release from a rupturing mature schizont-infected erythrocyte and invasion of new erythrocytes, merozoites are transiently exposed in the circulation, and are thus potentially vulnerable to attack by preventive measures based upon immunological or biochemical methods. To design such tools, it is important to understand the molecular composition of the merozoite and the structure-function makeup of the molecular interactions that occur as the merozoite recognizes and gains entry into a host cell.

Like most apicomplexan parasites, the malaria merozoite invades host cells via a multistep process initiated by reversible binding to the erythrocyte surface. Subsequently, a high affinity attachment occurs between the apical end of the merozoite and the host cell, followed by the movement of the junctional adhesion zone (moving junction) around the merozoite toward its posterior pole. Finally the merozoite invaginates into the erythrocyte by forming a nascent parasitophorous vacuole [2]. The moving junction is one of the most distinctive features of apicomplexan invasion and was first observed in

Abbreviations: aa, amino acid(s); Ab, antibody; AMA1, apical membrane antigen 1; GST, Glutathione S transferase; PBS, phosphate-buffered saline; PCR, polymerase chain reaction; RON, rhoptry neck protein.

☆ Sequence data from this article have been deposited with the GenBank™/EMBL/DDBJ databases under accession numbers AB444588–AB444592.

* Corresponding author. Department of Protozoology, Institute of Tropical Medicine (NEKKEN), Nagasaki University, Sakamoto, Nagasaki 852-8523, Japan. Tel.: +81 95 819 7838; fax: +81 95 819 7805.
E-mail address: okaneko@nagasaki-u.ac.jp (O. Kaneko).

1383-5769/$ – see front matter © 2008 Elsevier Ireland Ltd. All rights reserved.
doi:10.1016/j.parint.2008.09.005

Plasmodium species in the late 1970s [3], but the molecular nature of its structure remains unresolved.

Recent studies in *Toxoplasma gondii* suggest that host cell invasion involves protein discharge from at least two apical secretory organelles, the micronemes and rhoptries, based on the observation that a microneme protein, Apical Membrane Protein 1 (AMA1), forms a complex with three rhoptry neck (RON) proteins: RON2, RON4 and Ts4705 (RON5) [4–6]. These proteins have predicted orthologs in *P. falciparum*, and the RON4 ortholog has been reported to associate with *Pf*AMA1 [7] and to be localized at the moving junction [8], suggesting that the complex (and likely its function) is conserved between *T. gondii* and *P. falciparum* [7]. Attempts to knock-out the AMA1 gene locus were unsuccessful in both *Plasmodium* [9] and *T. gondii* [10], and the conditional reduction of *Tg*AMA1 expression severely impaired the cell invasion ability of *T. gondii* [11], indicating AMA1 has an essential function. The conservation of the RON proteins among apicomplexan parasites suggest that their functions and protein interactions are also conserved in the biology of host cell invasion. However, in *Plasmodium*, the details of this complex have yet to be fully characterized. In this study, to better understand the moving junction complex formation in *Plasmodium*, we sought to characterize *Pf*RON2 and determine the nature of its interaction with *Pf*RON4 and *Pf*AMA1.

2. Materials and methods

2.1. Malaria parasites

P. falciparum cloned lines 3D7, HB3, Dd2, 7G8, FVO, and D10 were maintained *in vitro*, essentially as previously described [12].

2.2. DNA and RNA isolation

Genomic DNA (gDNA) was isolated from *P. falciparum* using IsoQuick™ (Orca Research Inc., Bothell, WA). To determine transcription levels throughout the asexual stages, schizonts were purified by differential centrifugation on a 70%/40% Percoll-sorbitol gradient, after which released merozoites were allowed to invade uninfected erythrocytes for 4 h before the clearance of all remaining schizonts using 5% D-sorbitol. Fractions of the culture were harvested immediately and 24 h later, and then at 6 h intervals thereafter. Total RNA was isolated from parasite-infected erythrocytes stored at −20 °C in RNA*later*™ (Qiagen, Valencia, CA), using the RNeasy Mini Kit (Qiagen). Following DNase treatment, complementary DNA (cDNA) was generated with random hexamers using an Omniscript Reverse Transcription Kit (Qiagen).

2.3. Polymerase chain reaction (PCR) amplification and sequencing

A TBLASTN search was performed against the *P. falciparum* genome database (3D7 parasite line) via PlasmoDB website (http://www.plasmodb.org/) [13] using the *Tg*RON2 amino acid sequence as a query. To evaluate the polymorphism of *Pf*RON2, five pairs of overlapping primers were used for PCR amplification from HB3, FVO, Dd2, D10, and 7G8 parasite lines, and sequences were determined by direct sequencing of the PCR-amplified DNA fragments using an ABI PRISM® 3100-*Avant* Genetic Analyzer (Applied Biosystems, Foster City, CA). Oligonucleotides used were as follows: fRON2.F2 (5′-GATTCCAATAATTATAATTCTGATAATG-3′) and fRON2.R2 (5′-CGTAAAATATTCATTATATGAAAGATATGC-3′), fRON2.F3 (5′-GCATTAGGAGAACTTGTTGAACCA-3′) and fRON2.R3 (5′-CATAATATCTAAATAGGTTTTTGCTGAC-3′), fRON2.F4 (5′-GGATTAGTATTTTTATATGCAATGATTG-3′) and fRON2.R4 (5′-GTTATTTTCTAATAAATGTTTACTATCTTC-3′), fRON2.F5 (5′-GATAAATGGGATCAATTTATAAATAAGG-3′) and fRON2.R5 (5′-GCTAGCTACTGGTCCTGCACCT-3′), and fRON2.F6 (5′-ATGCAATTACCTTACTTAAGTCAAATG-3′) and fRON2.R6 (5′-ATATAAAATGAAAATAACAGAAAAGGTTATG-3′).

2.4. Quantification of pfron2 transcripts

Transcription of *ron2* was evaluated in the HB3 parasite line by real-time reverse transcription (RT)-PCR using a QuantiTect SYBR Green PCR Kit (Qiagen) and a LightCycler System (Roche, Basel, Switzerland). As a control, transcription of *ama1* and *rhoph2* was also evaluated. Oligonucleotides used were as follows: fRON2.qF (5′-CAGAACTAAGCAAACATGTAAAACATG-3′) and fRON2.qR (5′-GTATAACGCCTTGCTCATTTCCTG-3′) for *pfron2* (product size is 133 bp); fAMA1.qF (5′-GGAAGAGGACAGAATTATTGGGAAC-3′) and fAMA1.qR (5′-CCTGAATCTTCTTGTTGGTATGTATG-3′) for *pfama1* (product size is 137 bp); fRhopH2.qF (5′-GTAACAACACTTACTAAGGCAGACT-3′) and fRhopH2.qR (5′-GTACAAAGCTACAATATTGTTAGATCT-3′) for *pfrhoph2* (product size is 210 bp). The same oligonucleotides were used to PCR-amplify DNA fragments to be ligated into the pGEM-T Easy® plasmid (Promega, Madison, WI) which was used to make a standard curve to evaluate the copy number of each transcript.

2.5. Antibodies

A DNA fragment encoding amino acid positions (aa) 21–98 of *Pf*RON2 was PCR-amplified from *P. falciparum* 3D7 gDNA and ligated into pEU-E01GST-N2, an expression plasmid with N-terminal glutathione S transferase (GST)-tag followed by a PreScission Protease cleavage site, designed specifically for the wheat germ cell-free protein expression system (CellFree Sciences Co., Ltd., Matsuyama, Japan) [14], to produce recombinant GST-fused fRON2N protein (GST-fRON2N). Oligonucleotides used in the PCR amplification were fRON2.SalF1 (5′-*GTCGAC*TCAGAACTAAGCAAACATGTAAAACATG-3′) and fRON2.SalR1 (5′-*GTCGAC*CCCATTATTCATTTCACTACCAGGA-3′) (SalI restriction sites are underlined). Produced GST-fRON2N was captured using a glutathione-Sepharose 4B column and eluted with 10 mM reduced gluthathione, pH 8.0. To generate anti-*Pf*RON2 sera, BALB/c mice were immunized subcutaneously with 20 μg of purified GST-fRON2N emulsified with Freund's adjuvant. A Japanese white rabbit was immunized subcutaneously with 500 μg of purified GST-fRON2N with Freund's adjuvant for the first time, followed by 250 μg thereafter. All immunizations were done 4 times at 3 week intervals, prior to collection of antisera. Rabbit anti-*Pf*RhopH2 serum was obtained from I. Ling (National Institute for Medical Research, UK) [15], Rabbit anti-*Pf*AMA1 serum was obtained from C. Long (National Institute of Health, USA), and mouse monoclonal anti-*Pf*RON4 antibody (Ab; 26C64F12) was obtained from J.-F. Dubremetz (Université de Montpellier 2, France) [7]. Rabbit anti-Clag3.1 serum was as previously described [16].

2.6. SDS-PAGE and Western blot analysis

The recombinant protein, GST-fRON2N, was digested with a PreScission Protease at 4 °C overnight before analysis. Triton X-100 extracts of *P. falciparum* or recombinant proteins were dissolved in SDS-PAGE loading buffer, incubated at 100 °C for 3 min, and subjected to electrophoresis under reducing conditions on a 5–20% polyacrylamide gel (ATTO, Japan). Proteins were then transferred to a 0.22 μm PVDF membrane (BioRad, Hercules, CA). The proteins were immunostained with antisera followed by horseradish peroxidase-conjugated secondary Ab (Biosource Int., Camarillo, CA) and visualized with Immobilon™ Western Chemiluminescent HRP Substrate (Millipore, Billerica, MA) on RX-U film (Fuji, Japan). The relative molecular sizes of the parasite-encoded proteins were calculated by reference to molecular size standards (BioRad).

2.7. Immunoprecipitation

Immunoprecipitation was carried out as previously described [17]. Briefly, proteins were extracted from late schizont parasite pellets by

1% Triton X-100 treatment in phosphate-buffered saline (PBS) containing cOmplete Proteinase Inhibitor Cocktail Tablets (Roche). Supernatants (50 μl) were pre-incubated at 4 °C for 1 h with 20 μl of 50% protein G-conjugated beads (GammaBind Plus Sepharose; GE Healthcare) in NETT buffer (50 mM Tris–HCl, 0.15 M NaCl, 1 mM EDTA, and 0.5% Triton X-100) supplemented with 0.5% BSA (fraction V; Sigma-Aldrich). Recovered supernatants were incubated with rabbit antisera (anti-*Pf*RON2, anti-*Pf*AMA1, or anti-*Pf*RhopH2) or mouse anti-*Pf*RON4 Ab with gentle rotation at 4 °C for 2 h and then 20 μl of 50% protein G-conjugated beads were added. After 1 h incubation at 4 °C, the beads were washed once with NETT-0.5% BSA, once with NETT, once with high-salt NETT (0.5 M NaCl), once with NETT, and once with low-salt NETT (0.05 M NaCl and 0.17% Triton X-100). Finally, proteins were extracted from the protein G-conjugated beads by incubation with SDS-PAGE reducing loading buffer at 100 °C for 3 min. Supernatants were collected for Western blot analysis.

2.8. Indirect immunofluorescence assay

Thin smears of schizont-enriched *P. falciparum*-infected erythrocytes (Dd2 parasite line) were prepared on glass slides and stored at −80 °C. The smears were thawed, formaldehyde-fixed, and preincubated with PBS containing 5% non-fat milk at 37 °C for 30 min. They were then incubated with antisera at 37 °C for 1 h, followed by fluorescein isothiocyanate (FITC)-conjugated goat anti-(IgG and IgM) secondary Ab (Jackson ImmunoResearch Laboratories, West Grove, PA) and Alexa546-conjugated goat anti-(IgG and IgM) secondary Ab (Invitrogen, Carlsbad, CA) at 37 °C for 30 min. Nuclei were stained with 4′,6-diamidino-2-phenylindole (DAPI). Slides were mounted in ProLong Gold antifade reagent (Invitrogen) and viewed under oil-immersion. High resolution image-capture and processing were performed using a confocal scanning laser microscope (LSM5 PASCAL; Carl Zeiss MicroImaging, Thornwood, NY). Images were processed in Adobe Photoshop (Adobe Systems Inc., San José, CA).

2.9. Immunoelectron microscopy

Parasites were fixed for 15 min on ice in a mixture of 1% paraformaldehyde–0.1% glutaraldehyde in 0.1 M phosphate buffer (pH 7.4). Fixed specimens were washed, dehydrated, and embedded in LR White resin (Polysciences, Inc., Warrington, PA) as previously described [18,19]. Thin sections were blocked at 37 °C for 30 min in PBS containing 5% non-fat milk and 0.01% Tween 20 (PBS-MT). Grids were then incubated at 4 °C overnight with mouse anti-*Pf*RON2 or control sera in PBS-MT. After washing with PBS containing 10% BlockAce (Yukijirushi, Sapporo, Japan) and 0.01% Tween 20 (PBS-BT), the grids were incubated at 37 °C for 1 h with goat anti-mouse IgG conjugated to 10 nm gold particles (Amersham Life Science, Arlington, IL) diluted 1:20 in PBS-MT, rinsed with PBS-BT, and fixed on ice for 10 min in 2.5% glutaraldehyde to stabilize the gold. Then the grids were rinsed with distilled water, dried, and stained with uranyl acetate and lead citrate. Samples were examined with a transmission electron microscope (JEM-1230; JEOL Ltd., Tokyo, Japan).

2.10. Primary structure analysis of the protein

Signal peptide sequence was evaluated by SignalP3.0 [20]. Transmembrane region was evaluated by TMpred [21] and TMHMM2.0 [22]. Low complexity region was evaluated by Globplot 2.3 [23]. Amino acid sequence alignment was generated by MUSCLE [24].

2.11. Statistical analysis

Number of nonsynonymous substitutions over numbers of nonsynonymous sites (d_N), number of synonymous substitutions over numbers of synonymous sites (d_S), and their standard errors were computed using the Nei-Gojobori method with Jukes-Cantor correction implemented in MEGA 4.0.1 [25]. Standard errors were estimated using the bootstrap method with 500 replications. The statistical difference between d_N and d_S was tested using a one-tail *Z*-test with 500 bootstrap pseudosamples.

3. Results

3.1. RON2 orthologs of apicomplexan parasites

Using *Tg*RON2 as a query in BLAST analyses [26], and similar analyses using the predicted orthologs thus identified, we found RON2 orthologs in *P. falciparum* (*Pf*RON2; PF14_0495, PlasmoDB), *P. yoelii* 17XNL strain (*Py*RON2; PY06813, TIGR), *P. knowlesi* H strain (*Pk*RON2; PKH_125430 or PK14_2335w, Sanger Centre), and *P. vivax* Sal-I strain (*Pv*RON2; Pv117880, TIGR), *P. berghei* (*Pb*RON2; Contig5108), *P. chabaudi* (*Pch*RON2; Contig882.0), *Theileria annulata* (*Ta*RON2; Fig. S1A, TA19445 and TA19390, Sanger Centre [27]), *Theileria parva* (*Tp*RON2; Fig. S1B, TP01_0014, TIGR [28]), and *Babesia bigemina* (*Bbig*RON2; Fig. S1C, Contig3449, Sanger Centre). The RON2 were fragmented in the *P. berghei*, *P. chabaudi*, *T. annulata*, and *T. parva* genome nucleotide sequence databases, and full-length versions were constructed (supplementary Table S1).

3.2. PfRON2 protein structure and similarity to RhopH1/Clag proteins

The full-length *Pf*RON2 protein consists of 2189 residues with a putative signal peptide sequence at its N-terminus from amino acid positions (aa) 1 to 20. An interspecies variable region (aa 55–878), exhibiting low complexity and many repeats [23], was identified by comparing 6 *Plasmodium* RON2 amino acid sequences (Figs. 1 and S2). A BLASTP search using the conserved region of *Pf*RON2 (aa 879–2189) as a query identified *P. vivax* RhopH1/Clag homolog (XP_001616939.1, aa 251–394; E=0.001) as possessing homology with *Pf*RON2 aa 1105–1259. A Position-Specific Iterated BLAST search using *Pf*RON2 aa 1105–1259 as a query converged at iteration 3 and indentified most of the RhopH1/Clag genes in *Plasmodium* species. Alignment of RhopH1/Clag with RON2 from multiple genera identifies a predicted globular domain that is likely stabilized by disulfide bonds between 4 conserved Cys residues (Fig. 2). Three transmembrane regions were predicted by TMpred, however TMHMM2.0 predicted only a single transmembrane region for all *Plasmodium* RON2 orthologs assessed.. Interestingly, TMpred predicted a putative transmembrane region in the region conserved between RhopH1/Clag and RON2 (Fig. 2). Because RhopH1/Clag is a component of a soluble protein complex, we considered that these predicted transmembrane regions in RhopH1/Clag and RON2 constitute a likely hydrophobic region buried within a globular domain. Another predicted transmembrane region at aa 1114–1133 in *Pf*RON2 is also possibly hydrophobic region buried within a globular domain. TMpred considers the observation that there is an overrepresentation of positively charged amino acid

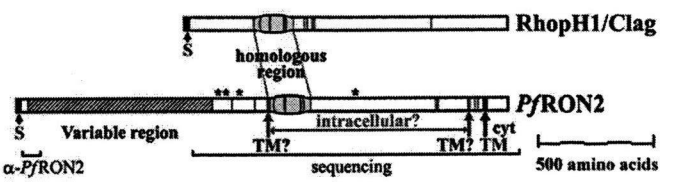

Fig. 1. Schematic representation of *Pf*RON2. S and TM indicate putative signal peptide (aa 1–20) and transmembrane sequences, respectively. The shaded box indicates an interspecies variable region. Vertical red bars indicate conserved Cys residues among orthologous sequences. Homologous region between RhopH1/Clag and RON2 is indicated by a yellow box. The region used to generate anti-*Pf*RON2 sera (α-*Pf*RON2) and the region sequenced in the laboratory lines (sequencing) are indicated. Asterisks indicate polymorphic sites.

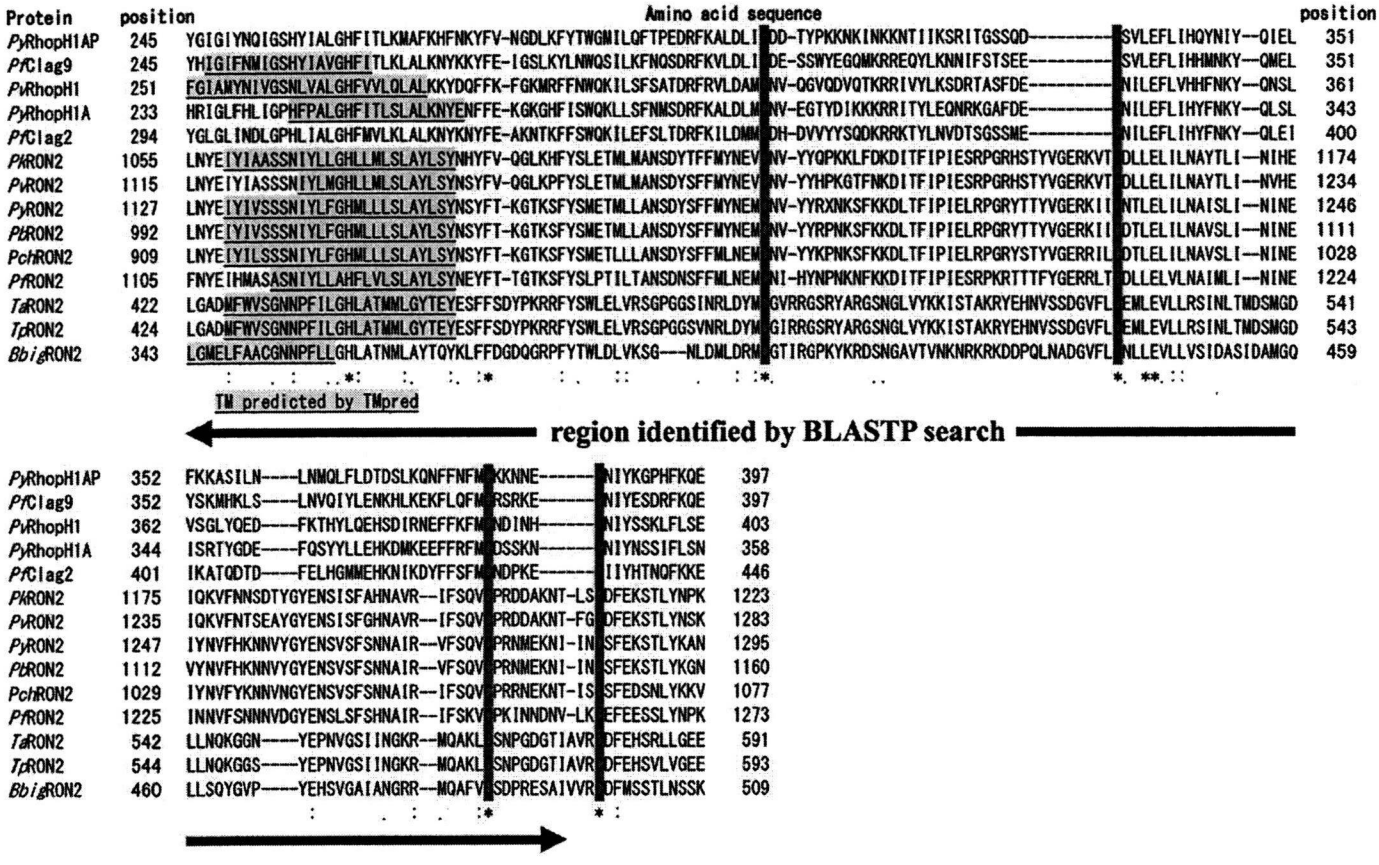

Fig. 2. Amino acid alignment of *Plasmodium* RON2 and RhopH1/Clag. Alignment was generated by MUSCLE [24] with manual correction. "*" indicates that the residues in that column are identical in all sequences in the alignment. ":" indicates conserved substitutions and "." indicates semi-conserved substitutions. In addition to 9 RON2 sequences, *P. falciparum* Clag2 (AAC71977), Clag9 (CAD52032), *P. yoelii* RhopH1A (BAB70675), RhopH1AP (BAB70677), and *Pv*RhopH1 (contig 1047) were used to generate the alignment. Cys residues are highlighted in red. The region possessing homology between RhopH1/Clag and RON2 as identified by BLASTP is indicated by the bar under the alignment.

residues in the cytoplasmic loops of the transmembrane protein [21], which is a likely explanation for this discrepancy.

3.3. *PfRON2 transcription peaks at the schizont stage*

To determine the transcription pattern in the asexual stages of the parasite life-cycle, quantitative RT-PCR was performed on the HB3 parasite line prepared from a synchronized culture harvested at 6 h intervals. Both RON2 and AMA1 transcriptions were seen to peak around 36–40 h after invasion, when parasites were in the schizont stage. AMA1 showed a broader and flatter transcription peak than RON2 (Fig. 3). Transcriptome data compiled in the PlasmoDB website [13,29] also indicated a milder wave crest of AMA1 transcripts compared with RON2.

3.4. *Complex formation of PfRON2, PfRON4, and PfAMA1*

Mouse and rabbit anti-*Pf*RON2 sera were generated using recombinant GST-fRON2N. Firstly, we evaluated the reactivity of anti-*Pf*RON2 sera by Western blot using recombinant proteins. Both antisera recognized the fRON2N component of the recombinant protein after cleavage (Fig. S3, filled arrows). Cleaved 26.4-kDa GST component (Fig. S3, arrowheads) and 46-kDa GST-fused PreScission protease (Fig. S3, unfilled arrow) were also recognized by these Abs.

Secondly, we evaluated the reactivity of these sera against native RON2 proteins extracted from schizont stage *P. falciparum* (HB3 line) by Western blot analysis. Both antisera reacted with a band slightly larger than 250 kDa (Fig. 4A, arrows), which is similar to the predicted molecular weight of *Pf*RON2 after exclusion of the putative signal peptide sequence (247 kDa). An 80-kDa band was detected by both mouse and rabbit antisera in HB3 extract, for which the exact identity is not known, but a possible processed product of *Pf*RON2. A 55-kDa band detected with rabbit antiserum was also detected with preimmune serum, suggesting that this band was unrelated to

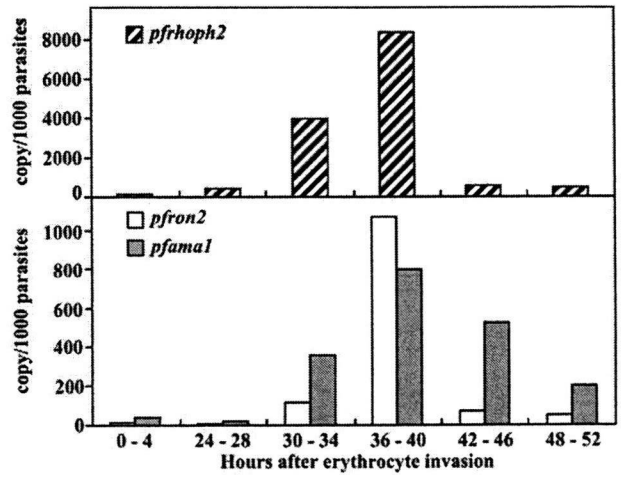

Fig. 3. Transcriptional analysis by quantitative RT-PCR of *pfrhoph2*, *pfron2*, and *pfama1* genes during blood stages of *P. falciparum* (HB3 line). Y-axis indicates copy number of each transcript detected per 1000 parasites. Similar results were observed in 3 independent experiments (data not shown).

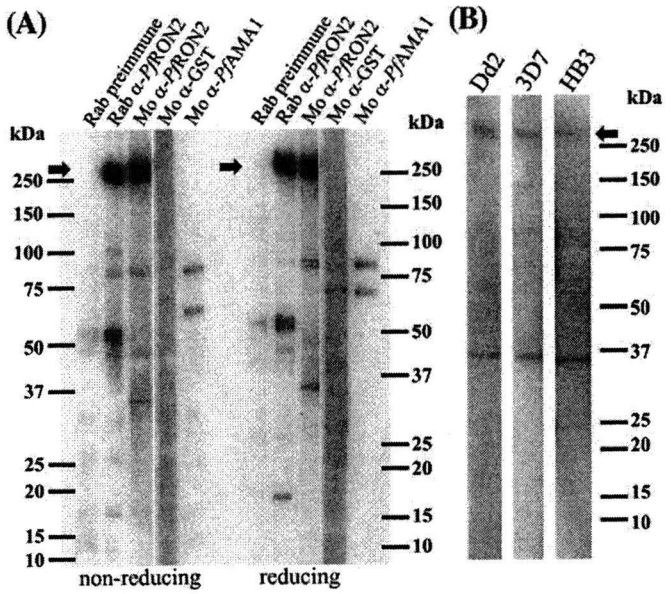

Fig. 4. Western blot analysis of antisera against native parasite proteins. (A) Schizont-enriched parasite extracts were stained by rabbit preimmune serum, (Rab preimmune), rabbit anti-*Pf*RON2 (Rab α-*Pf*RON2), mouse anti-fRON2N (Mo α-*Pf*RON2), and Abs against GST (Mo α-GST) or *Pf*AMA1 (Mo α-*Pf*AMA1) under both reducing and non-reducing conditions. Both mouse and rabbit anti-*Pf*RON2 sera detected a band slightly larger than 250 kDa. (B) Western blot of schizont-enriched parasite extracts from 3 different *P. falciparum* lines, Dd2, 3D7, and HB3 with mouse anti-fRON2N serum. Arrows indicate predicted *Pf*RON2 bands.

*Pf*RON2. A 35-kDa band was detected with mouse antiserum but not with rabbit antiserum, suggesting that it is also unrelated to RON2.

To evaluate the interaction between *Pf*RON2, *Pf*RON4, and *Pf*AMA1, we performed immunoblotting against immunoprecipitated materials from mature schizont-rich parasite extracts (Fig. 5). We found that RON2 was detected in the precipitated fraction using anti-*Pf*AMA1 or anti-*Pf*RON4. In the reciprocal experiment, *Pf*AMA1 and *Pf*RON4 were also detected in the precipitated fraction of anti-*Pf*RON2 serum. Although it is theoretically possible that such immunoprecipitated fractions contained the *Pf*RON2-*Pf*RON4, *Pf*RON2-*Pf*AMA1, and *Pf*RON4-*Pf*AMA1 dimeric complexes as appropriate to the primary

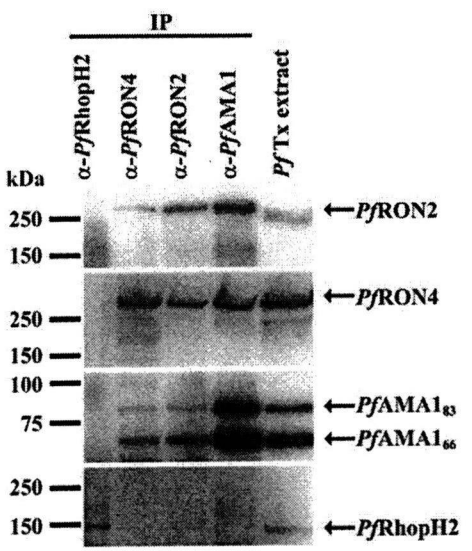

Fig. 5. *Pf*RON2 is co-precipitated with *Pf*RON4 and *Pf*AMA1. Schizont-rich parasite Triton X-100 extracts (*Pf* Tx extract) were immunoprecipitated (IP) with rabbit sera against *Pf*RhopH2 (α-*Pf*RhopH2), *Pf*RON2 (α-*Pf*RON2), *Pf*AMA1 (α-*Pf*AMA1) or mouse monoclonal Ab against *Pf*RON4 (α-*Pf*RON4), then stained against *Pf*RON2, *Pf*AMA1, *Pf*RON4, or *Pf*RhopH2. $AMA1_{83}$ is a proprotein form and $AMA1_{66}$ is a processed form.

antibody, considering that these 3 proteins are distinct molecules that do not possess any similarity each other, this specific co-immunoprecipitation suggests complex formation among *Pf*RON2, *Pf*RON4, and *Pf*AMA1 in *P. falciparum*. The fact that both the 83-kDa proform and the 66-kDa processed form were co-precipitated with *Pf*RON2 indicated that a region responsible for complex formation was located in the 66-kDa form of AMA1 [30]. Neither of these was detected in the anti-RhopH2 immunoprecipitate, thereby excluding not only the possibility of *Pf*RON2 involvement in the RhopH complex, but also potential carryover due to insufficient or inadequate washing steps.

3.5. RON2 is expressed at the rhoptry neck of Plasmodium merozoites

Dual labeling indirect immunofluorescent assay was performed using anti-*Pf*RON2 with either anti-*Pf*AMA1 (microneme marker), anti-Clag3.1 (rhoptry body marker), or anti-*Pf*RON4 (rhoptry neck marker) antibodies in order to determine the sub-cellular location of *Pf*RON2 in *P. falciparum* (Fig. 6). In segmented schizonts, RON2 antisera produced a punctate pattern of fluorescence and each developing merozoite showed a single small punctate *Pf*RON2-positive signal located at the apical end. Although some parts of the *Pf*RON2 signal

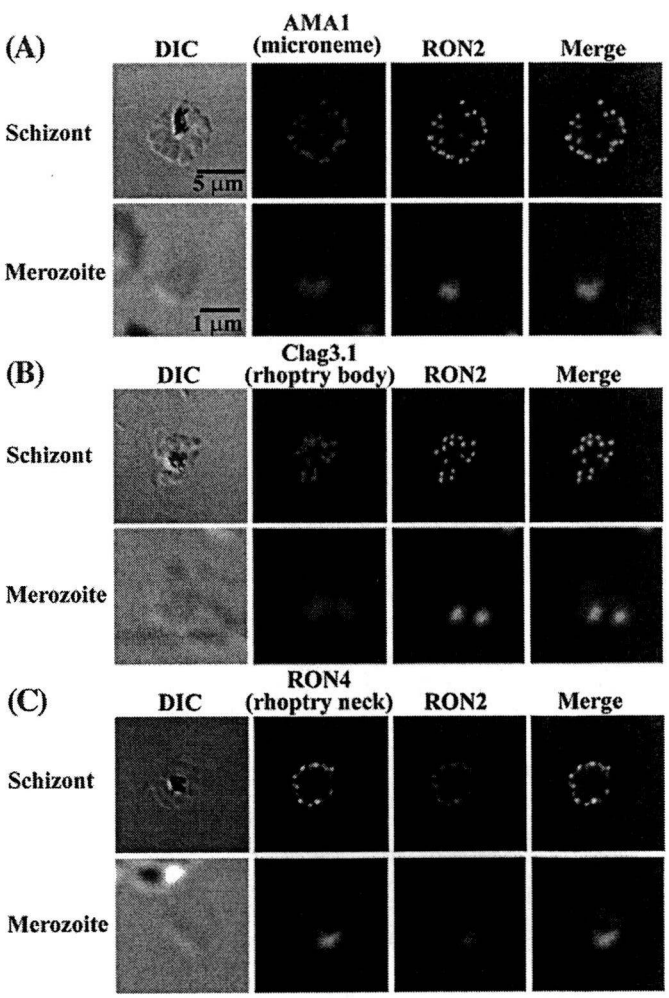

Fig. 6. *Pf*RON2 is expressed at the apical end of *Plasmodium* merozoites. Schizont-infected erythrocytes and merozoites were dual-labeled with antisera against *Pf*RON2 and *Pf*AMA1 (A), *Pf*Clag3.1 (B), or *Pf*RON4 (C). Merged images are shown in the right panels. All segmented schizonts and merozoites are positive for *Pf*RON2. Nuclei are counterstained with DAPI. Colocalization of *Pf*RON2 with *Pf*RON4 (rhoptry neck marker) was observed but neither colocalized with *Pf*Clag3.1 (rhoptry body marker) nor *Pf*AMA1 (microneme marker). To eliminate the background staining, negative control sera were always used and images were assessed (data not shown).

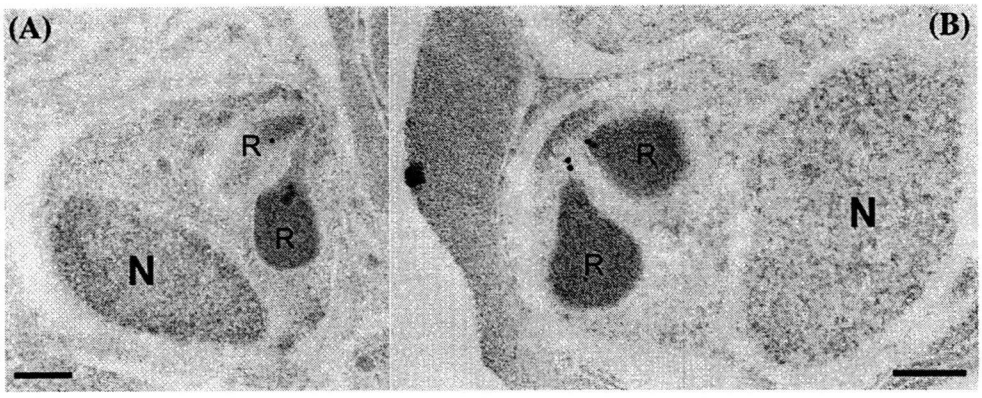

Fig. 7. Rhoptry neck localization of *Pf*RON2 by immunoelectron microscopy. Longitudinally sectioned merozoites in schizont-infected erythrocytes were labeled with anti-*Pf*RON2 serum followed by secondary Ab conjugated with gold particles. Gold particles were restricted to the narrow neck portion of the rhoptries (R). Two different images are shown (A and B). N indicates nucleus. Bars = 200 nm.

overlapped with microneme protein AMA1 and rhoptry body protein Clag3.1, it did not colocalize well with those markers, whereas complete colocalization was observed with the rhoptry neck marker *Pf*RON4.

Immunoelectron microscopy was carried out to determine the precise localization of the protein. *Pf*RON2 was detected in the neck portion of the pear-shaped rhoptries in segmented schizonts (Fig. 7). Thus *Pf*RON2 is seen to compartmentalize in the rhoptry neck.

3.6. Potential positive diversifying selection on *PfRON2*

To evaluate the polymorphic nature of *Pf*RON2, we sequenced the *pfron2* nucleotide sequence (2459–6570), excluding the 5′ low complexity region, in 5 *P. falciparum* parasite lines and compared them with the sequence from the genome database (3D7 line). A total of 5 nonsynonymous nucleotide substitutions were observed at nucleotide positions 2615, 2710, 2914, 4391 and 4392, resulting 4 amino acid substitutions (Table 1). An excess of nonsynonymous substitutions ($d_N = 0.0007 \pm 0.0003$) over synonymous substitutions ($d_S = 0.0002 \pm 0.0002$) was detected ($P = 0.0333$), indicating *Pf*RON2 is subject to positive diversifying selection.

4. Discussion

In this study, we characterized *P. falciparum* RON2 for its protein structure, transcription profiles, intracellular localization, and complex formation with *Pf*RON4 and *Pf*AMA1.

*Pf*RON2 possesses a region harboring homology with another rhoptry protein RhopH1/Clag, a component of the RhopH complex that possesses erythrocyte binding ability [16,31,32]. Co-immunoprecipitation showed that *Pf*RON2 does not form a complex with RhopH2, suggesting that *Pf*RON2 is unlikely to be a component of the RhopH complex. Because RON2 orthologs can be found in other apicomplexan parasites and RhopH1/Clag is found only in *Plasmodium* species, RhopH1/Clag probably evolved via acquisition of a conserved functional domain from RON2 during its generation in *Plasmodium* species. Thus, this homologous region may have a common function between these two complexes. The sequence of *Tg*RON2 deposited to the database (GenBank accession number DQ096563) only possesses the C-terminal half of the conserved region between RON2 and RhopH1/Clag. By comparing *Tg*RON2 gDNA and cDNA sequences, we noticed that intron 3 is relatively large (2272 bp) and contains a potential sequence encoding the N-terminal portion of the conserved region. Thus it is possible that there is another alternatively spliced transcript encoding the full length of the conserved region. Alternatively, it is also possible that this region represents an ancient vestigial exon.

Interestingly, we could readily detect complex formation between AMA1 and RON proteins in the extract obtained from mature schizont-rich parasites, suggesting that complex formation had already occurred at the schizont stage likely at the apical end upon secretion of RON proteins from rhoptry and AMA1 from microneme. This is in contrast to the other apicomplexa parasite *T. gondii*, in which the AMA1-RON complex was proposed to form at the initial contact with the host cell. The precise timing of the complex formation is not clear, but may vary depending on the parasite species. Among RON proteins characterized thus far, only *Tg*RON4 was visualized to locate at the moving junction during cell invasion. Whether *Pf*RON2 and *Pf*RON4 locate at the moving junction and whether the complex remains intact during cell invasion are still need to be clarified. We found that *Pf*RON2 degraded more rapidly than *Pf*RON4 after extraction (Fig. S4), which may explain the previous observation by Alexander et al. (2006), who did not detect *Pf*RON2 in the immunoprecipitant with anti-*Pf*AMA1 Ab [7].

The association between the 83-kDa proform of *Pf*AMA1 with RON proteins raises the possibility that the processing of *Pf*AMA1 from the 83-kDa form to 66-kDa form occurs not only in the microneme, as previously proposed [33], but also on the apical tip of the merozoite after release from the microneme in mature schizonts. If this is the case, it is not clear whether this AMA1 processing occurs after complex formation with RON proteins or is mainly achieved prior to this. However, it is formally possible that disruption of the different intracellular microorganelles during the experimental procedure resulted in an artificial complex formation of *Pf*AMA1 proform, for which further studies are required.

Due to the fact that *P. falciparum* AMA1 exhibits relatively high polymorphism between lines, which is considered to be generated by positive diversifying selection under the human immune pressure, we evaluated the polymorphic nature of *Pf*RON2. Although the level of polymorphism of RON2 is not high, the fact that $d_N > d_S$ suggests that positive diversifying selection does indeed act on RON2. Three types of

Table 1
Nucleotide and amino acid polymorphism of *Pf*RON2

Nucleotide positions (amino acid) [a]	Parasite line					
	3D7	7G8	HB3	Dd2	FVO	D10
2614–2616	tCa (Ser)	tCa (Ser)	tCa (Ser)	tCa (Ser)	tCa (Ser)	tTa (Leu)
2710–2712	Cat (His)	Cat (His)	Cat (His)	Tat (Tyr)	Tat (Tyr)	Tat (Tyr)
2914–2916	Gac (Asp)	Gac (Asp)	Cac (His)	Gac (Asp)	Gac (Asp)	Gac (Asp)
4390–4392	gAA (Glu)	gAA (Glu)	gAC (Asp)	gGC (Gly)	gGC (Gly)	gAA (Glu)

[a] Nucleotide numbering is after the 3D7 line sequence.

amino acid substitutions found at aa 1464 (Asp, Glu, and Gly) suggests that this particular site is under diversifying selection and is possibly to be exposed to host immunity. Thus, *Pf*RON2 not only appears to have an important role in host cell invasion by apicomplexan parasites, but also is a potential target for malaria intervention strategies.

Acknowledgements

We thank N Iyoku for her expertise, I Ling for anti-*Pf*RhopH2 serum, C Long for anti-*Pf*AMA1 serum, anti-*Pf*RON4 antibody (26C64F12) for J-F Dubremetz, and R Culleton for critical reading. Preliminary sequence data of *P. knowlesi*, *P. berghei*, *P. chabaudi*, and *B. bigemina* were produced by the corresponding groups at the Sanger Institute website at http://www.sanger.ac.uk/. Preliminary sequence data of *P. vivax* was produced at the Institute for Genomic Research website at http://www.tigr.org. This work was supported in part by Grants-in-Aid for Scientific Research 17590372 and 17406009 (to OK) from the Ministry of Education, Culture, Sports, Science and Technology, Japan. JC acknowledges the support of National Natural Science Foundation of China 30700695.

Appendix A. Supplementary data

Supplementary data associated with this article can be found, in the online version, at doi:10.1016/j.parint.2008.09.005.

References

[1] Snow RW, Guerra CA, Noor AM, Myint HY, Hay SI. The global distribution of clinical episodes of *Plasmodium falciparum* malaria. Nature 2005;434:214–7.
[2] Kaneko O. Erythrocyte invasion: vocabulary and grammar of the *Plasmodium* rhoptry. Parasitol Int 2007;56:255–62.
[3] Aikawa M, Miller LH, Johnson J, Rabbege J. Erythrocyte entry by malarial parasites. a moving junction between erythrocyte and parasite. J Cell Biol 1978;77:72–82.
[4] Boothroyd JC, Dubremetz JF. Kiss and spit: the dual roles of *Toxoplasma* rhoptries. Nat Rev Microbiol 2008;6:79–88.
[5] Alexander DL, Mital J, Ward GE, Bradley P, Boothroyd JC. Identification of the moving junction complex of *Toxoplasma gondii*: a collaboration between distinct secretory organelles. PLoS Pathog 2005;1:e17.
[6] Lebrun M, Michelin A, El Hajj H, Poncet J, Bradley PJ, Vial H, et al. The rhoptry neck protein RON4 re-localizes at the moving junction during *Toxoplasma gondii* invasion. Cell Microbiol 2005;7: 1823–33.
[7] Alexander DL, Arastu-Kapur S, Dubremetz JF, Boothroyd JC. *Plasmodium falciparum* AMA1 binds a rhoptry neck protein homologous to TgRON4, a component of the moving junction in *Toxoplasma gondii*. Eukaryot Cell 2006;5:1169–73.
[8] Baum J, Tonkin CJ, Paul AS, Rug M, Smith BJ, Gould SB, et al. A malaria parasite formin regulates actin polymerization and localizes to the parasite-erythrocyte moving junction during invasion. Cell Host Microbe 2008;3:188–98.
[9] Triglia T, Healer J, Caruana SR, Hodder AN, Anders RF, Crabb BS, et al. Apical membrane antigen 1 plays a central role in erythrocyte invasion by *Plasmodium* species. Mol Microbiol 2000;38:706–18.
[10] Hehl AB, Lekutis C, Grigg ME, Bradley PJ, Dubremetz JF, Ortega-Barria E, et al. *Toxoplasma gondii* homologue of *Plasmodium* apical membrane antigen 1 is involved in invasion of host cells. Infect Immun 2000;68:7078–86.
[11] Mital J, Meissner M, Soldati D, Ward GE. Conditional expression of *Toxoplasma gondii* apical membrane antigen-1 (TgAMA1) demonstrates that TgAMA1 plays a critical role in host cell invasion. Mol Biol Cell 2005;16:4341–9.
[12] Trager W, Jensen JB. Human malaria parasites in continuous culture. Science 1976;193:673–5.
[13] Bahl A, Brunk B, Crabtree J, Fraunholz MJ, Gajria B, Grant GR, et al. PlasmoDB: the *Plasmodium* genome resource. a database integrating experimental and computational data. Nucleic Acids Res 2003;31:212–5.
[14] Tsuboi T, Takeo S, Iriko H, Jin L, Tsuchimochi M, Matsuda S, et al. The wheat germ cell-free based production of malaria proteins for discovery of novel vaccine candidates. Infect Immun 2008;76:1702–8.
[15] Ling IT, Kaneko O, Narum DL, Tsuboi T, Howell S, Taylor HM, et al. Characterisation of the *rhoph2* gene of *Plasmodium falciparum* and *Plasmodium yoelii*. Mol Biochem Parasitol 2003;127:47–57.
[16] Kaneko O, Yim Lim BY, Iriko H, Ling IT, Otsuki H, Grainger M, et al. Apical expression of three RhopH1/Clag proteins as components of the *Plasmodium falciparum* RhopH complex. Mol Biochem Parasitol 2005;143:20–8.
[17] Kaneko O, Fidock DA, Schwartz OM, Miller LH. Disruption of the C-terminal region of EBA-175 in the Dd2/Nm clone of *Plasmodium falciparum* does not affect erythrocyte invasion. Mol Biochem Parasitol 2000;110:135–46.
[18] Torii M, Adams JH, Miller LH, Aikawa M. Release of merozoite dense granules during erythrocyte invasion by *Plasmodium knowlesi*. Infect Immun 1989;57: 3230–3.
[19] Aikawa M, Atkinson CT. Immunoelectron microscopy of parasites. Adv Parasitol 1990;29:151–214.
[20] Bendtsen JD, Nielsen H, von Heijne G, Brunak S. Improved prediction of signal peptides: signalP 3.0. J Mol Biol 2004;340:783–95.
[21] Hofmann K, Stoffel W. TMbase — a database of membrane spanning proteins segments. Biol Chem Hoppe-Seyler 1993;374:166.
[22] Krogh A, Larsson B, von Heijne G, Sonnhammer EL. Predicting transmembrane protein topology with a hidden Markov model: application to complete genomes. J Mol Biol 2001;305:567–80.
[23] Linding R, Russell RB, Neduva V, Gibson TJ. GlobPlot: exploring protein sequences for globularity and disorder. Nucleic Acids Res 2003;31:3701–8.
[24] Edgar RC. MUSCLE: multiple sequence alignment with high accuracy and high throughput. Nucleic Acids Res 2004;32:1792–7.
[25] Tamura K, Dudley J, Nei M, Kumar S. MEGA4: Molecular Evolutionary Genetics Analysis (MEGA) software version 4.0. Mol Biol Evol 2007;24:1596–9.
[26] Altschul SF, Madden TL, Schäffer AA, Zhang J, Zhang Z, Miller W, et al. Gapped BLAST and PSI-BLAST: a new generation of protein database search programs. Nucleic Acids Res 1997;25: 3389–402.
[27] Pain A, Renauld H, Berriman M, Murphy L, Yeats CA, Weir W, et al. Genome of the host-cell transforming parasite *Theileria annulata* compared with *T. parva*. Science 2005;309:131–3.
[28] Gardner MJ, Bishop R, Shah T, de Villiers EP, Carlton JM, Hall N, et al. Genome sequence of *Theileria parva*, a bovine pathogen that transforms lymphocytes. Science 2005;309:134–7.
[29] Le Roch KG, Zhou Y, Blair PL, Grainger M, Moch JK, Haynes JD, et al. Discovery of gene function by expression profiling of the malaria parasite life cycle. Science 2003;301:1503–8.
[30] Howell SA, Withers-Martinez C, Kocken CH, Thomas AW, Blackman MJ. Proteolytic processing and primary structure of *Plasmodium falciparum* apical membrane antigen-1. J Biol Chem 2001;276:31311–20.
[31] Ghoneim A, Kaneko O, Tsuboi T, Torii M. The *Plasmodium falciparum* RhopH2 promoter and first 24 amino acids are sufficient to target proteins to the rhoptries. Parasitol Int 2007;56:31–43.
[32] Rungruang T, Kaneko O, Murakami Y, Tsuboi T, Hamamoto H, Akimitsu N, et al. Erythrocyte surface glycosylphosphatidyl inositol anchored receptor for the malaria parasite. Mol Biochem Parasitol 2005;140:13–21.
[33] Healer J, Triglia T, Hodder AN, Gemmill AW, Cowman AF. Functional analysis of *Plasmodium falciparum* apical membrane antigen 1 utilizing interspecies domains. Infect Immun 2005;73:2444–51.

Parasitology International 58 (2009) 101–105

Contents lists available at ScienceDirect

Parasitology International

journal homepage: www.elsevier.com/locate/parint

Short communication

Pyruvate kinase type-II isozyme in *Plasmodium falciparum* localizes to the apicoplast

Takuya Maeda [a,1], Tomoya Saito [a], Omar S. Harb [b], David S. Roos [b], Satoru Takeo [c], Hiroko Suzuki [c], Takafumi Tsuboi [c], Tsutomu Takeuchi [a], Takashi Asai [a,*]

[a] Department of Tropical Medicine and Parasitology, School of Medicine, Keio University, 35 Shinanomachi, Shinjuku-ku, Tokyo 160-8582, Japan
[b] Department of Biology, University of Pennsylvania, 301 Goddard Laboratories Philadelphia, PA 19104, USA
[c] Cell-Free Science and Technology Research Center, Ehime University, 3 Bunkyo-cho, Matsuyama, Ehime 790-8577, Japan

ARTICLE INFO

Article history:
Received 16 July 2008
Received in revised form 15 October 2008
Accepted 18 October 2008
Available online 31 October 2008

Keywords:
Plasmodium falciparum
Pyruvate kinase II
Apicoplast
Mitochondria
Cell-free expression

ABSTRACT

Bioinformatics research on *Plasmodium falciparum* revealed two isoforms of pyruvate kinase: type-I and type-II enzymes. The type-I enzyme shows typical glycolytic properties, while type-II enzyme is involved in fatty acid type-II biosynthesis and has been predicted to localize to the apicoplast with the targeting signal in its N-terminus. The type-I and type-II isoforms have the same evolutionary origin as *Toxoplasma gondii* isozymes, *Tg*PyKI and *Tg*PyKII, respectively; however, *Tg*PyKII localizes to both the mitochondrion and the apicoplast. Accordingly, we made a recombinant full length of *P. falciparum* pyruvate kinase type-II protein using a wheat germ cell-free expression system and obtained a specific antibody against the type-II protein. Fluorescent microscopic analysis revealed that *P. falciparum* type-II enzyme was localized only to the apicoplast, not to the mitochondrion. The data suggest differences in localization and metabolic pathways between *P. falciparum* and *T. gondii* pyruvate kinase isoforms.

Pyruvate kinase (EC 2.7.1.40) catalyzes the essentially irreversible transphosphorylation of phosphoenolpyruvate (PEP) to ADP. The activities of most mammalian and bacterial pyruvate kinases are allosterically regulated by fructose 1,6-bisphosphate, and pyruvate kinase is known to play a regulatory role in glycolysis. The glycolytic end product, pyruvate, feeds into various metabolic pathways, and hence pyruvate kinase is important in several primary metabolic reactions.

Many organisms have pyruvate kinase isozymes with different kinetic properties, and most pyruvate kinases in eukaryotes are reported to be located in the cytosol. Two types of pyruvate kinase were characterized in *Toxoplasma gondii* [1,2]. Pyruvate kinase type-II isozyme (*Tg*PyKII) was localized in both the mitochondrion and the apicoplast, whereas pyruvate kinase type-I (*Tg*PyKI) was located in the cytosol. *Tg*PyKII exhibited only 18% overall amino acid identity with *Tg*PyKI and showed novel properties of exhibiting high pH optima and GDP dependency [2].

The malaria bioinformatics website (http://sites.huji.ac.il/malaria/), compiled and maintained by Hagai Ginsburg, reports two isoforms of pyruvate kinase in *Plasmodium falciparum*. The type-I enzyme (*Pf*PyKI) has been characterized enzymologically in detail [3]. The type-II enzyme (*Pf*PyKII) was predicted to have an apicoplast targeting signal in the N-terminus; however, experimental localization has not been confirmed. Phylogenetic analysis indicated that *Pf*PyKI and *Pf*PyKII have the same evolutionary origin as *Tg*PyKI and *Tg*PyKII, respectively, suggesting that type-II has a proteobacterial origin [2]. Thus, we questioned whether both *Pf*PyKII and *Tg*PyKII are localized in both the apicoplasts and the mitochondria.

In this study, we made recombinant *Pf*PyKII protein in a wheat germ cell-free expression system, purified the recombinant protein, created an antibody, and localized *Pf*PyKII by immunofluorescent microscopy.

The *Pf*PyKII gene was amplified from *P. falciparum* genomic DNA. The two primers were 5′-ACTGGATCCCCATATTGCCTATGAT-3′ and 5′-TCGGGATCC CTAATTTGTTAGACATGG-3′ (*Bam*HI site is underlined). The first denaturation at 95 °C was for 10 min and each of 30 reaction cycles consisted of 94 °C for 30 s, 47 °C for 30 s, and 65 °C for 2 min, and a final elongation cycle step at 65 °C for 5 min using KOD-plus DNA polymerase (Toyobo Co. Ltd, Osaka, Japan). Thereafter, the amplified DNA products were treated with *Bam*HI and inserted into a plasmid pEU-E01G-N2 (Cell-Free Science and Technology Research Center, Ehime University, Ehime, Japan) using the LigaFast ligation kit (Promega, Madison, WI, USA) according to the manufacturer's protocol. The plasmid was electroporated into the *Escherichia coli* DH10B (Takara Bio, Kyoto, Japan) and the bacteria were grown in a plate. The right directional clones were detected by DNA sequencing using the ABI PRISM BigDye terminator cycle sequencing kit (Applied Biosystems, Foster, CA, USA) and loaded onto an ABI PRISM 310 DNA sequencer. After plasmid purification

* Corresponding author. Tel.: +81 3 3353 1211x62747; fax: +81 3 3353 5958.
E-mail address: asait@sc.itc.keio.ac.jp (T. Asai).
[1] Present address: International Research Center for Infectious Diseases, The Institute of Medical Science, The University of Tokyo, Shiroganedai 4-6-1, Minato-ku, Tokyo 108-8639, Japan.

1383-5769/$ – see front matter © 2008 Elsevier Ireland Ltd. All rights reserved.
doi:10.1016/j.parint.2008.10.005

using Qiagen Plasmid Midi Kit (Qiagen, Hilden, Germany), the plasmid was further purified by C_5Cl_2 ultra-centrifugation at 391,000 ×g for 16 h at 25 °C to avoid endotoxin contamination. The purified plasmid containing a glutathione S-transferase (GST) coding region and an SP6 promoter upstream of the DNA inserted region was treated with SP6 RNA polymerase (GE Healthcare, Little Chalfont, Buckinghamshire, UK). The method of mRNA production and translation in wheat germ was described previously [4].

The GST-pyruvate kinase isozyme fusion protein in the wheat germ extract was purified using an affinity column of glutathione sepharose 4B (GE Healthcare). The pyruvate kinase isozyme was cut from the fusion protein by PreScission Protease (GE Healthcare) according to

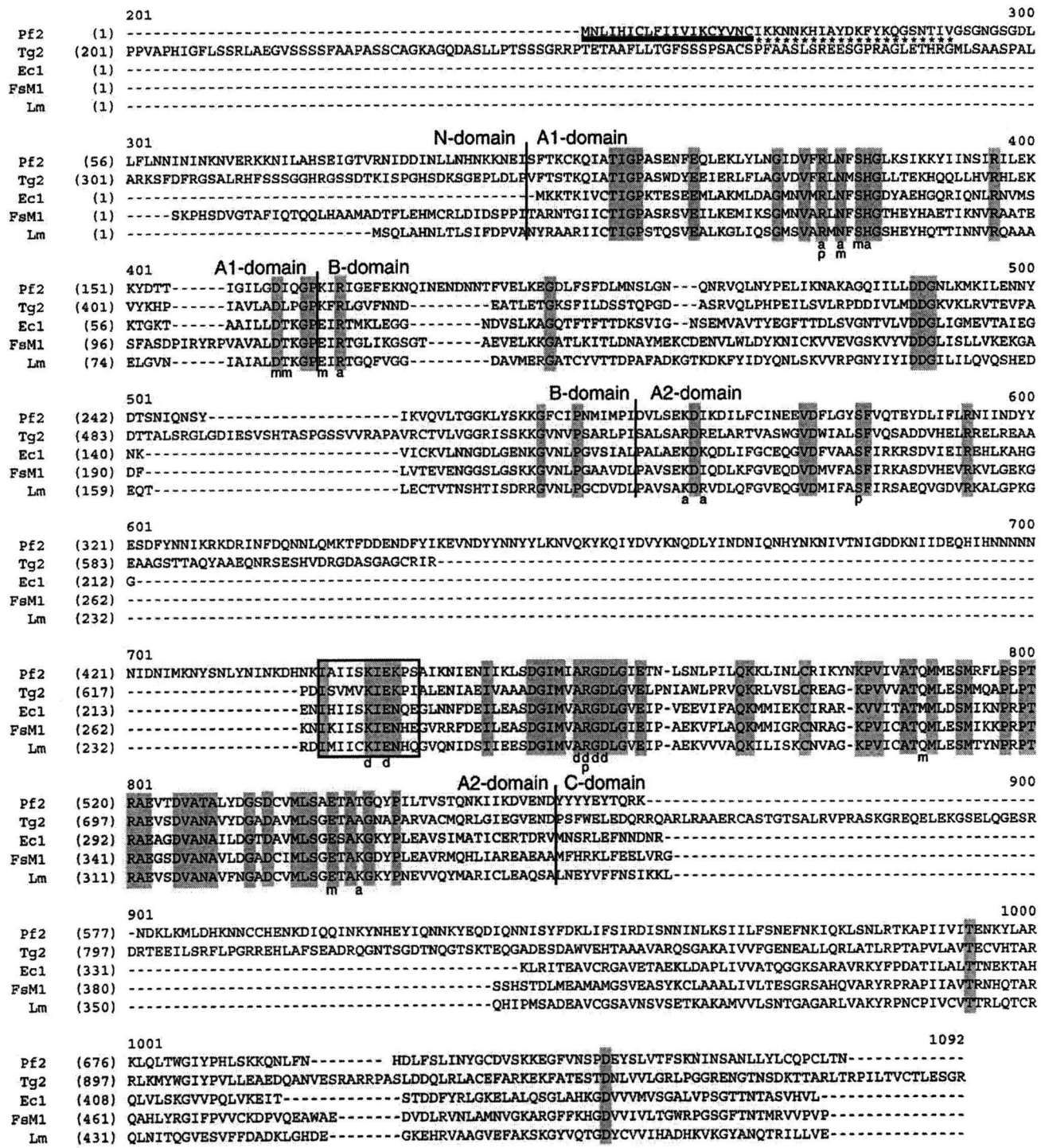

Fig. 1. Amino acid sequence alignment of *P. falciparum* pyruvate kinase type-II isozyme (*Pf*PyKII) with four pyruvate kinases from other species. Sequence data accession numbers are: Pf2, *Pf*PyKII (this study; PF10_0363); Tg2, *Toxoplasma gondii* II (AB118155); Ec1, *Escherichia coli* isozyme I (1PKY_A); FsM1, *Felis catus* isozyme M1 (P11979); Lm, *Leishmania mexicana* (CAA52898). *Vertical lines* indicate divisions between four three-dimensional domains (N, A, B, and C) as described previously [10]. An open black *box* indicates the pyruvate kinase signature sequence (PROSITE, PS00110); *p* indicates PEP binding sites; *a*, ADP binding sites; *d*, divalent cation binding sites; *m*, monovalent cation binding sites; *dashes*, gaps in the alignment. DNA sequences analyses were performed using the VectorNTI suite (InforMax, Executive Way Frederick, MD, USA). The thick underline in the N-terminal of *P. falciparum* sequence is signal sequence, and following asterisks indicates probable plastid transit peptide. It is conceivable that these sequences compose apicoplast targeting signal. Targeting signals in the N-terminal were analyzed by SignalP [11] and PlasmoAP [12].

the manufacturer's recommendations. Pyruvate kinase isozyme purity was analyzed by SDS–PAGE on 8% polyacrylamide gel as described by Laemmli [5] (Data not shown). The recombinant protein concentration was determined by Bradford assay [6] using bovine serum albumin (BSA) as a standard.

Anti-recombinant *Pf*PyKII antibody was produced through a commercial company (Immuno-Biological Laboratories, Takasaki, Japan). Briefly, purified recombinant *Pf*PyKII from wheat germ extracts was used to immunize a BALB/c mouse. Following six injections of pyruvate kinase isozyme (5 μg each) at 1-week intervals, the whole IgG was isolated from peritoneal fluid with a HiTrap rProtein A FF column (GE Healthcare). The whole cell lysate of 1×10^8 erythrocytic stage *P. falciparum* parasites (FCR-3 strain) was separated on 8% acrylamide gel and blotted onto a nitrocellulose Hybond-C Extra membrane (GE Healthcare). The membrane was blocked for 20 min with 2% skimmed milk in Tris-buffered saline containing 0.2% Tween 20, incubated for 1 h with primary antibodies (1:3000), probed with alkaline phosphatase-conjugated goat anti-mouse IgG (Vector Laboratories, Burlingame, CA, USA) (1:5000), and detected with a BCIP-NBT system (Roche, Basel, Switzerland). Molecular sizes of the protein bands were determined with reference to pre-stained Rainbow molecular weight markers (GE Healthcare).

Cells were fixed and stained using the procedures described by Tonkin et al. [7]. Cells were briefly fixed with 4% EM grade paraformaldehyde (ProSciTech, Thuringowa, Queensland, Australia) and 0.0075% EM grade glutaraldehyde (ProSciTech) in phosphate-buffered saline (PBS) for 30 min. Fixed cells were washed once in PBS and permeated with 0.1% Triton X-100/PBS for 10 min. Cells were washed again and treated with 0.1 mg/ml of sodium borohydride ($NaBH_4$)/PBS for 10 min. Following another wash, cells were blocked in 3% BSA/PBS for 1 h. For staining anti-*Pf*PyKII antibody-binding structure and apicoplast, anti-*Pf*PyKII mouse antibody (diluted 1/1000) and anti-acyl carrier protein (ACP) rabbit antibody (diluted 1/500; gifted by Geoff McFadden, University of Melbourne, Australia) were added and allowed to bind for a minimum of 1 h in 3% BSA/PBS. AlexaFluor goat anti-mouse 594 (red) and anti-rabbit 488 (green) secondary antibodies (Invitrogen, Carlsbad, CA, USA) were added at 1:1000 dilution (in 3% BSA/PBS) and allowed to bind for 1 h, while cells settled onto a previously flamed cover slip coated with 1% polyethylenimine (PEI; Sigma, St Louis, MO, USA). For staining the anti-*Pf*PyKII antibody-binding structure and mitochondrion, citrate synthase-GFP construct (gifted by Geoff McFadden) transformed *P. falciparum* was used. Anti-*Pf*PyKII mouse antibody (diluted 1/1000) was added and allowed to bind for 1 h, followed by addition of AlexaFluor goat anti-mouse 488 (green) antibody and Cy5-conjugated anti-GFP rabbit (red) antibody (diluted 1/1000; Sigma) and allowed to bind for 1 h. Cells were mounted in 50% glycerol with 0.1 mg/ml of 1,4-diazabicyclo[2,2,2]octane (DABCO, Sigma). The microscopic system was a DeltaVision restoration system (Applied Precision, Washington, USA) on an Olympus IX70 inverted microscope equipped with a mercury vapor lamp (100 W) and appropriate barrier emission filters. Images were taken 0.2 μm apart and deconvolved using softWoRx Explorer Suite (Applied Precision).

The deduced amino acid sequence of *Pf*PyKII (NCBI Accession# NP_700836), exhibiting low overall identity (21%) to that of *Pf*PyKI (NCBI Accession# CAG25081), contained a pyruvate kinase signature (PROSITE; PS00110) as did other species and other consensus regions, such as multiple binding sites of ADP, PEP, and divalent cations (Fig. 1). Based on protein alignment, *Pf*PyKII was predicted to be a monovalent cation-independent enzyme. Most of the monovalent cation-binding sites were conserved; however, two binding sites, Thr^{113} and Glu^{117} (in *Felis catus* pyruvate kinase), were substituted by Ile and Lys, respectively. These substitutions are a common characteristic of monovalent cation-independent pyruvate kinases. We found three-specific long insertions in the middle of domain B, A2, and C of *Pf*PyKII, as in *Tg*PyKII. These insertions were different in length, but the insert positions were the same as in *Tg*PyKII.

Following six injections of pyruvate kinase isozyme at 1-week intervals, the whole IgG was isolated from mouse peritoneal fluid. Western blot analysis showed a single band (~80 kDa) in the *P. falciparum* lysate (Fig. 2), which was different from the mass in the type-I enzyme (55.6 kDa), indicating no cross-reaction with the type-I enzyme. Preimmune serum detected no bands in the 1×10^8 *P. falciparum* lysate (data not shown). The antibody was used in immunofluorescence microscopy.

The stained structure from the anti-*Pf*PyKII antibody in *P. falciparum* merged into the apicoplast stained pattern (Fig. 3A), suggesting that *Pf*PyKII localizes to the apicoplast. To determine if *Pf*PyKII localizes to the mitochondria, we analysed the immunolocalization of *Pf*PyKII in a *P. falciparum* cell line expressing the citrate synthase fused to GFP, which targets to the mitochondria [7] (Fig. 3B). The merged image showed that anti-*Pf*PyKII stain is adjacent to, but not associated with, the mitochondria. The two stains were distinguishable in all the stages (data not shown). Thus, we concluded that *Pf*PyKII localizes to the apicoplast, not to the mitochondrion. The data indicate a different localization of type-II pyruvate kinase in *P. falciparum* from that in *T. gondii*.

A recombinant protein of *P. falciparum* pyruvate kinase type-II isozyme (*Pf*PyKII) was created using a wheat germ cell-free system. All our previous attempts for production of this recombinant protein in *E. coli* systems have failed. Probably, it was due to its biased codon usage. The efficiency of production of the protein in our study was not high; nevertheless, the wheat germ cell-free system is useful for creation of the recombinant protein.

In addition, we showed localization of *Pf*PyKII in the apicoplast by immunofluorescent assay. Despite its proteobacterial origin, *Pf*PyKII was localized only to the apicoplast, not to the mitochondrion as in *Tg*PyKII, which is localized to both the mitochondrion and the apicoplast. The difference in metabolic pathways in the organelles between *T. gondii* and *P. falciparum* might reflect differences in their internal environment and in the metabolic relationships between those organelles in the two parasites. Further investigation to reveal these potential differences will contribute to understanding survival of *T. gondii* and *P. falciparum* in the host.

As suggested by Ralph et al. [8], pyruvate kinase in the apicoplast might dephosphorylate PEP imported into the apicoplast via PEP transporter on the apicoplast membrane and supply pyruvate for fatty acid synthesis and the non-mevalonate 1-deoxy-D-xylulose-5-phophate (DOXP) pathway in the organelle. Fleige et al. [9], reporting on carbohydrate metabolism in the *T. gondii* apicoplast, indicated that *Tg*PykII was localized in the apicoplast. These findings suggest differences between *T. gondii* and *P. falciparum* in the mitochondrion and apicoplast metabolic pathways, even though *T. gondii*

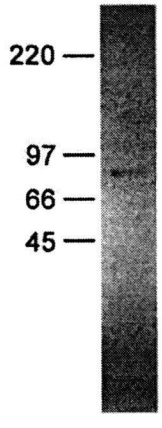

Fig. 2. Specificity of anti-*Pf*PyKII IgG shown by Western blot analysis. The purified recombinant *Pf*PyKII was detected by Western blot analysis with the antibody against the recombinant *Pf*PyKII. Rainbow molecular weight markers (kDa) are indicated on the left.

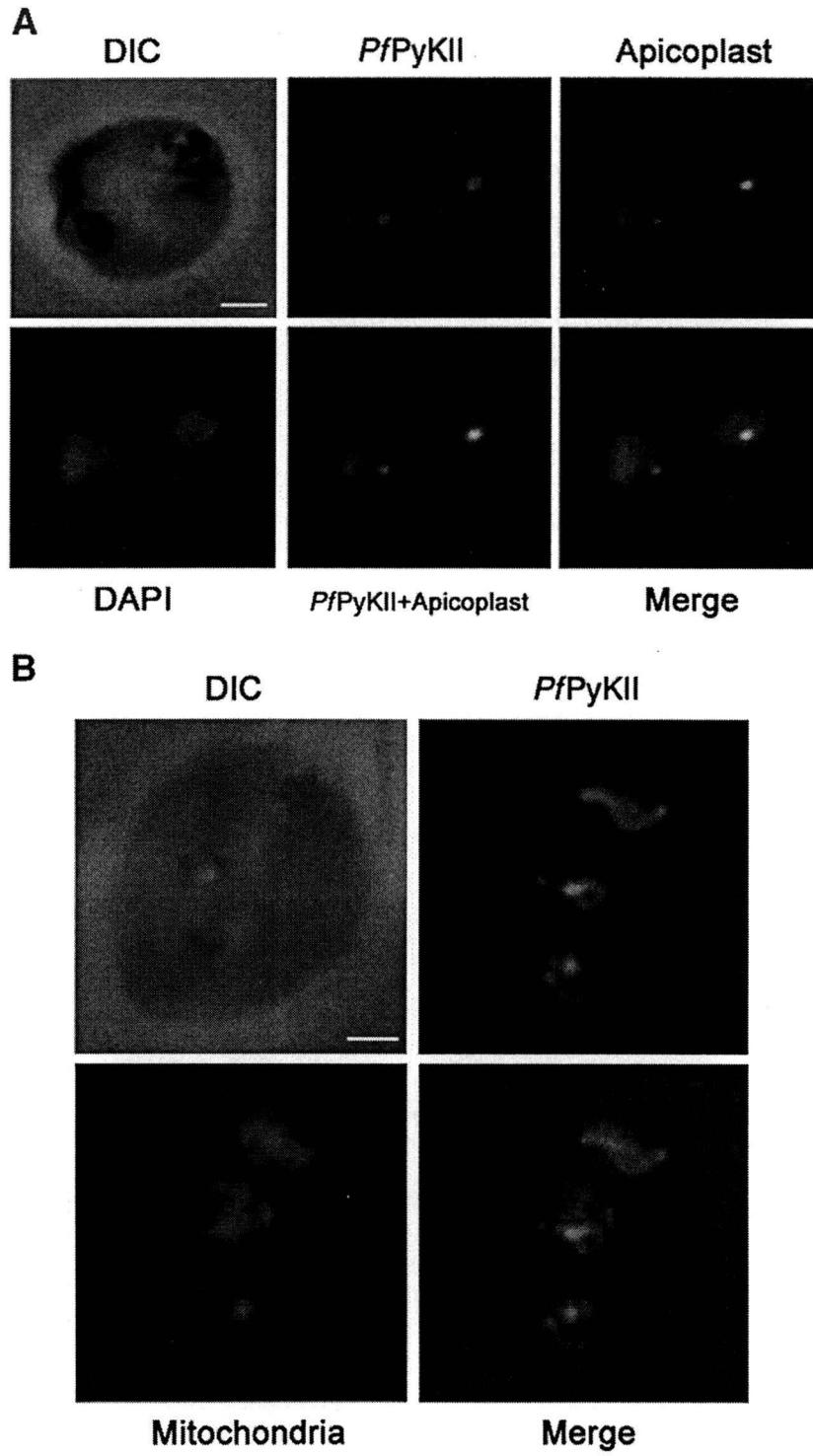

Fig. 3. Immunofluorescent microscopic analysis of co-localization of *Pf*PyKII with the apicoplast, but not with the mitochondrion in red blood cells infected with *P. falciparum*. A: Anti-*Pf*PyKII and anti-*P. falciparum* ACP antibodies detected by AlexaFlour goat anti-mouse 594 (red) and goat anti-rabbit 488 (green) secondary antibodies, respectively. Immunofluoresecnce of *P. falciparum* ACP antibody shows the apicoplast. Merged images indicate co-localization of *Pf*PyKII and *P. falciparum* ACP. Nucleus stained by DAPI (blue). B: Red blood cells infected with parasites expressing citrate synthase fused to GFP targeting the mitochondrion (Tonkin et al. 2004). GFP detected by Cy5-conjugated goat anti-GFP (red). Anti-*Pf*PyKII antibody detected by AlexaFluor goat anti-mouse 488 (green) IgG. Merged image shows that *Pf*PyKII does not co-locate with the mitochondrion. White scale bars are 2 μm.

and *P. falciparum* have comparable organelle components, and were thought to have similar enzyme components in both the apicoplast and the mitochondrion. The pathway differences might reflect differences in intracellular environments or different abilities to import metabolites into those organelles. We expected that the difference in enzymatic properties between *Tg*PyKII and *Pf*PyKII would help in understanding their roles in the two parasites, but several attempts to express the active recombinant enzyme have failed. As pyruvate kinase has been thought to play a role only in glycolysis in the cytosol, pyruvate kinases localized with cell organelles are unique. Non-glycolytic pyruvate kinases have been found only in the apicomplexan parasites, such as *Plasmodium* sp,

Theileria sp, and *T. gondii*. Characterization of non-glycolytic pyruvate kinases would increase the understanding of the unique metabolic pathways in protozoan parasites.

In addition to uncertainty about metabolic pathways, we are also uncertain about the origin of *Pf*PyKII. Although *Pf*PyKII exhibits a typical bipartite signal in the N-terminus, *Pf*PyKII has a proteobacterial origin, which is indicative of the apicoplast protein, and not a cyanobacterial or plastidic origin [2]. We suggest that *Pf*PyKII might have been obtained from endosymbiotic bacteria. Originally *Pf*PyKII may have localized in both the mitochondrion and the apicoplast, as in *T. gondii*; subsequently *P. falciparum* may have lost the mitochondrial location during evolutionary development.

Acknowledgements

We thank Dr. Shinichiro Kawazu (Obihiro University of Agriculture and Veterinary Medical) for providing genomic DNA of *P. falciparum*, and Dr. Geoffrey I. McFadde (University of Melbourne) for providing both anti-acyl carrier protein rabbit antibody and *P. falciparum* expressing citrate synthase fused to GFP. This work was supported in part by Keio Gijuku Academic Development Funds, Japan.

References

[1] Maeda T, Saito T, Oguchi Y, Nakazawa M, Takeuchi T, Asai T. Expression and characterization of recombinant pyruvate kinase from *Toxoplasma gondii* tachyzoites. Parasitol Res 2003;89:259–65.
[2] Saito T, Nishi M, Lim MI, Wu B, Maeda T, Hashimoto H, Takeuchi T, Roos DS, Asai T. A novel GDP-dependent pyruvate kinase isozyme from *Toxoplasma gondii* localizes to both the apicoplast and the mitochondrion. J Biol Chem 2008;283:14041–52.
[3] Chan M, Sim TS. Functional analysis, overexpression, and kinetic characterization of pyruvate kinase from *Plasmodium falciparum*. Biochem Biophys Res Commun 2004;326:188–96.
[4] Sawasaki T, Gouda MD, Kawasaki T, Tsuboi T, Tozawa Y, Takai K, Endo Y. The wheat germ cell-free expression system: methods for high-throughput materialization of genetic information. Methods Mol Biol 2005;310:131–44.
[5] Laemmli UK. Cleavage of structural proteins during the assembly of the head of bacteriophage T4. Nature 1970;227:680–5.
[6] Bradford MM. A rapid and sensitive method for the quantitation of microgram quantities of protein utilizing the principle of protein–dye binding. Anal Biochem 1979;72:248–54.
[7] Tonkin CJ, van Dooren GG, Spurck TP, Struck NS, Good RT, Handman E, Cowman AF, McFadden GI. Localization of organellar proteins in *Plasmodium falciparum* using a novel set of transfection vectors and a new immunofluorescence fixation method. Mol Biochem Parasitol 2004;137:13–21.
[8] Ralph SA, van Dooren GG, Waller RF, Crawford MJ, Fraunholz MJ, Foth BJ, Tonkin CJ, Roos DS, McFadden GI. Tropical infectious diseases: metabolic maps and functions of the *Plasmodium falciparum* apicoplast. Nat Rev Microbiol 2004;2:203–16.
[9] Fleige T, Fischer K, Ferguson DJP, Gross U, Bohne W. Carbohydrate metabolism in the *Toxoplasma gondii* apicoplast: localization of three glycolytic isoenzymes, the single pyruvate dehydrogenase complex, and a plastid phosphate translocator. Eukaryot Cell 2007;6:984–96.
[10] Rigden DJ, Phillips SE, Michels PA, Fothergill-Gilmore LA. The structure of pyruvate kinase form *Leishmania mexicana* reveals details of the allosteric transition and unusual effector specificity. J Mol Biol 1999;291:615–35.
[11] Bendtsen JD, Nielsen H, von Heijne G, Brunak S. Improved prediction of signal peptides: SignalP 3.0. J Mol Biol 2004;340:783–95.
[12] Foth BJ, Ralph SA, Tonkin CJ, Struck NS, Fraunholz M, Roos DS, Cowman AF, McFadden GI. Dissecting apicoplast targeting in the malaria parasite *Plasmodium falciparum*. Science 2003;299(5607):705–8.

Parasitology International 58 (2009) 196–199

Contents lists available at ScienceDirect

Parasitology International

journal homepage: www.elsevier.com/locate/parint

Short communication

A small-scale systematic analysis of alternative splicing in *Plasmodium falciparum*

Hideyuki Iriko [a,b,c], Ling Jin [a,b], Osamu Kaneko [d,e], Satoru Takeo [b], Eun-Taek Han [b,f], Mayumi Tachibana [d], Hitoshi Otsuki [d], Motomi Torii [d], Takafumi Tsuboi [a,b,*]

[a] *Venture Business Laboratory, Ehime University, Matsuyama, Ehime 790-8577, Japan*
[b] *Cell-Free Science and Technology Research Center, Ehime University, Matsuyama, Ehime 790-8577, Japan*
[c] *Department of Microbiology and Pathology, Faculty of Medicine, Tottori University, Yonago, Tottori 683-8503, Japan*
[d] *Department of Molecular Parasitology, Ehime University Graduate School of Medicine, Toon, Ehime 791-0295, Japan*
[e] *Department of Protozoology, Institute of Tropical Medicine (NEKKEN), Nagasaki University, Sakamoto, Nagasaki 852-8523, Japan*
[f] *Department of Parasitology, Kangwon National University College of Medicine, Chunchon 200-701, Republic of Korea*

ARTICLE INFO

Article history:
Received 6 November 2008
Received in revised form 30 January 2009
Accepted 15 February 2009
Available online 5 March 2009

Keywords:
Alternative splicing
Exon definition
Gametocyte
Malaria
Plasmodium falciparum

ABSTRACT

During the last decade transcriptome analyses demonstrated that alternative splicing plays an important role to generate a large number of mRNA and protein isoforms from a limited number of genes. However, the frequency of the alternative splicing dramatically varies among living organisms. For example, 35–65% of human genes are involved in alternative splicing, whereas only a few are reported for unicellular organism yeast. Alternative splicing has been observed for several genes in the deadliest malaria parasite *Plasmodium falciparum*, but the frequency and the type were not systematically analyzed so far. In this study, we determined partial cDNA sequences for 88 open reading frames surrounding 246 introns in *P. falciparum* which were transcribed at schizont and gametocyte stages, and observed 15 instances of alternative splicing within a total of 14 gene transcripts, 16% of the analyzed genes. Among 5 basic splicing patterns, alternative 5′ and 3′ splicing, and intron retention were detected. Alternative splicing in 7 open reading frames had effects on the domain architectures of the gene products, which might result in modifying the cellular localization and function of these products.

Malaria is a significant human disease of global concern that causes several million deaths annually, as well as hundreds of millions of episodes of clinical illness. The intricate life cycle of the pathogenic protozoan agent of malaria, *Plasmodium*, belays an extraordinary biological complexity that underlies its development in both a warm-blooded host and mosquito vector. The parasite has the capacity to recognize and infect multiple cell types, such as salivary glands, hepatocytes, and erythrocytes; and has three distinct motile or invasive stages that traverse different tissues before infecting a new host cell [1]. In comparison to the simple unicellular yeasts, which are predicted to have ~5000 genes [2], the estimated size of the *Plasmodium* genome appears to inadequately reflect the remarkable biological complexity of its life cycle. The *Plasmodium falciparum* genome is estimated to have ~6000 genes, and the complexity of unique genes is considerably less due to the amplification of numerous multi-gene families, such as *var*, *rif*, and *stevor* [3], that occupy a significant part of the *Plasmodium* genome.

During the last decade transcriptome analyses demonstrated that alternative splicing plays an important role to generate a large number of mRNA and protein isoforms from a limited number of genes [4,5]. However, the frequency of the alternative splicing dramatically varies among living organisms. For example, 35–65% of human genes are involved in alternative splicing, whereas only a few are reported for yeast [4], despite the observation of 4730 predicted introns that are encoded within *Schizosaccharomyces pombe* genes [2]. In *P. falciparum*, 7406 introns were predicted in the genome, whereas alternative splicing has been observed only for a few genes that might affect protein function. For example, adenylyl cyclase variant isoforms may have functional differences [6]; and MAEBL variant isoforms are suggested to change the type I membrane product to a soluble isoform [7]. Another example is the stromal-processing peptidase and delta-aminolevulinic acid dehydratase, which share a common apicoplast-targeting leader sequence via the skipping of 4 intervening exons [8]. Alternative splicing was also reported for the blood stage antigen 41-3 precursor [9]; CDK-related protein kinase 6 [10]; and an aspartyl protease [11]. Thus, alternative splicing does occur in *Plasmodium*; however, the information is largely anecdotal and the prevalence of this mechanism remains unclear. Since alternative splicing can profoundly affect estimations of the breadth and complexity of the proteome (mRNA sequences) from the genome nucleotide sequence information, algorithms predictive of alternative splicing are increasingly needed. Indeed, we have observed in *P. falciparum* that alternatively spliced transcripts are not as rare as the anecdotal evidence would suggest, in the course of our experiences performing high-throughput cloning of protein expression constructs using cDNA templates [12]. In this report, we summarize our data and

Abbreviations: ORF, open reading frame.

* Corresponding author. Venture Business Laboratory, Ehime University, Matsuyama, Ehime 790-8577, Japan. Tel.: +81 89 927 8277; fax: +81 89 927 9941.
E-mail address: tsuboi@ccr.ehime-u.ac.jp (T. Tsuboi).

1383-5769/$ – see front matter © 2009 Elsevier Ireland Ltd. All rights reserved.
doi:10.1016/j.parint.2009.02.002

assess the frequency and the type of alternative splicing in *P. falciparum*; and predict the effect of altered transcripts on the localization and function of the produced proteins. Moreover, we provide evidence that the protozoan *P. falciparum* possesses both exon- and intron-recognition systems that initiate intron splicing.

The *P. falciparum* NF54 line was maintained in culture as described [13]. Asynchronous parasites were collected, and the erythrocytes were removed by saponin-mediated lysis. Parasite pellets were washed with phosphate buffered saline, and stored at −80 °C until use. Gametocyte stages were induced by maintaining parasite cultures at 37 °C using a gas mixture (90% N_2, 5% O_2, and 5% CO_2) for an extended period of time without the addition of fresh erythrocytes, and fully matured gametocytes were collected, washed in phosphate buffered saline, and stored at −80 °C until use. Sixty-nine % of the parasites were fully matured stage V gametocytes. Total RNA was extracted from parasite pellets using the RNeasy mini kit (Qiagen, Valencia, CA), and RNA preparations were extensively treated with DNase I to remove contaminating DNA. cDNA was prepared using Superscript III reverse-transcriptase (RT; Invitrogen, Carlsbad, CA). Open reading frames (ORFs) transcribed at schizont and gametocyte stages were selected for the analysis based on the transcriptome analysis [14]. Oligonucleotide primers were designed based upon annotated sequences in PlasmoDB [15], in order to PCR amplify predicted full-length ORFs. Eighty-eight ORFs were amplified by RT-PCR and cloned into the pCR2.1-TOPO TA plasmid (Invitrogen). Nucleotide sequence of the inserts were determined for 2 to 8 clones for each ORF using an ABI PRISM® 310 and 3100 Genetic Analyzers (Applied Biosystems, Foster City, CA) with M13(-20) and M13 reverse primers.

In this manner we randomly determined partial cDNA sequences for 88 ORFs surrounding 246 introns. The distribution of the ORFs arranged according to stage-specificity of the transcriptional cluster [14] and the number of the constituent introns are described in greater detail in Table 1. Similar to most other eukaryotes, exon boundaries of *Plasmodium* are demarcated by consensus donor and acceptor splicing junctions, GU and AG, respectively [16]. We observed 15 instances of alternative splicing within a total of 14 gene transcripts, 16% of the analyzed 88 genes (Table 1 and Supplementary Table 1). Because we only sequenced 2 to 8 clones for each intron, this value should be taken as a minimal estimation, and the true frequency of the alternative splicing is expected to be higher. To evaluate the alternative splicing in other strain, we performed RT-PCR analysis using gametocyte pellet purified from a malaria patient blood obtained from malaria endemic area in Mae Sot, Thailand. We checked 7 genes specifically expressed at gametocyte stage (PFE0220w, MAL8P1.149, MAL13P1.85, MAL13P1.211, PFD0700c, PF13_0220, and PFE0680w). As a result, five genes (PFE0220w, MAL8P1.149, MAL13P1.85, PFD0700c, and PF13_0220) also showed alternatively spliced variants together with the predicted parent transcripts as NF54 (data not shown). These results suggest that alternative splicing also occur in naturally isolated *P. falciparum* parasites. It was shown that alternative splicing in *P. falciparum* is a higher level than expected, based on the rarity of alternative splicing events in *S. pombe* [4].

The observed alternative splicing events were classified into 3 types: alternative 5′ splicing (46.7% of cases); alternative 3′ splicing (26.7% of cases); and intron retention/creation (26.7% of cases) (Fig. 1A). Notably, this is the first evidence of alternative 5′ splicing in *P. falciparum*. Another type of alternative splicing is exon skipping, which is the most prominent splicing pattern in metazoans; for example, 38% of events in humans are due to exon skipping [4,5]. Although 3 cases of exon skipping have been reported in *P. falciparum* [6,8,9], we did not observe this type occurring in this study.

Table 1
Analyzed *Plasmodium falciparum* introns in this study.

Cluster[a]	Stage[b]	Total		Alternative splicing	
		ORFs	Introns	ORFs (%)	Introns (%)
3	Gm	42	160	8 (19.0%)	9 (6.0%)
4	R/Sch/Mz	16	18	2 (12.5%)	2 (11.8%)
13	Sch/Gm	2	2	0 (0.0%)	0 (0.0%)
14	Spz/Sch/Gm	6	13	2 (33.3%)	2 (15.4%)
15	Sch	22	53	2 (9.1%)	2 (3.8%)
Total		88	246	14 (16.0%)	15 (6.4%)

[a] Open reading frames (ORF) were clustered based on the transcription pattern [14].
[b] Gm, gametocyte; R, ring; Sch, schizont; Mz, merozoite; Spz, sporozoite.

To assess the effect of the predicted alternative protein products, we analyzed the domain architectures of the splicing variants. Alternative splicing in 7 ORFs (MAL13P1.211, PFE0220w, PF13_0220, PF10_0021, PFD0700c, PF14_0694, and PFI0110c) had effects on the domain architectures of the gene products (Fig. 1B). The predicted parent transcripts (type 1) of MAL13P1.211 and PFE0220w encode proteins which possess a single transmembrane domain at their C-termini; whereas the alternatively spliced products harbored a frameshift and an early stop codon that resulted in truncated proteins lacking transmembrane domains. The cellular localization is therefore likely to depend on the splicing status, and the presence or absence of a transmembrane domain. Other transcripts (type 1) corresponding to PFD0700c, PF14_0694, and PFI0110c possessed at their C-termini an RNA recognition motif, thioredoxin motif, and protein kinase domain, respectively; whereas alternatively spliced variants (type 2) lacked these domains either partially or completely, suggesting that the protein functions would be abolished or suppressed. Although no known functional domains were detected for PF13_0220 or PF10_0021, the type 2 transcripts encode stop codons approximately 20 to 30 amino acids from the start codon, indicating that their expression as mature forms would be abolished.

Interestingly, among the two types of transcripts showing 5′ alternative splicing in *P. falciparum* the transcripts that encoded truncated product (type 2) almost always possessed a splicing site at the 5′ side compared to the predicted parent transcripts (type 1). This suggests that splicing site at 3′ side is original and that a cryptic splice site was activated in the preceding exon, likely weak splicing signal of the original site. In unicellular eukaryote yeast, mutations in splice sites lead to the activation of cryptic splice sites located downstream of the mutated site, suggesting that splicing machineries initially recognize intron (intron definition) [17]. However, in the metazoans, mutations in splice sites typically lead to the activation of cryptic splice sites located in the preceding exon or exon skipping [18], suggesting that the exon is primarily recognized (exon definition). Thus the pattern observed for *P. falciparum* fits to the "exon definition". Furthermore, 3 cases of exon skipping reported in *P. falciparum* support the presence of the "exon definition" system in this protist [6,8,9]. Because the observed intron retentions suggest the presence of "intron definition" system, *P. falciparum* appears to initiate splicing via both "exon definition" and "intron definition" systems. This is similar to the metazoan, *Drosophila melanogaster*, for which both intron retention and exon skipping have been observed [19,20].

In this study, we found frequent 5′ alternative splicing, however this type has never been reported in *P. falciparum* despite well over a decade of molecular cloning history of numerous *P. falciparum* genes. This might be explained by our cloning strategy to target gametocyte transcripts rather than asexual stage transcripts (Fig. 1). Because the *Plasmodium* female gametocyte was shown to translationally repress specific mRNA species by forming a complex in the cytoplasm to store mRNA for translation after fertilization [21], there might be a relation between these two observations via mRNA binding proteins. In all eukaryotes, splicing is mediated by a macromolecular spliceosome machinery that consists of small nuclear ribonucleoproteins (snRNPs) and non-snRNP splicing factors with RNA binding motif, including serine–arginine-rich (SR) proteins. Among SR proteins, SF2/ASF shows multiple functions, one of which is to affect alternative splice site selection by antagonizing other SR proteins, such as SC35 and SRp20 [22,23]. SF2/ASF is also reported to associate with ribosomes to stimulate translation [24]. Such concerted regulation of nuclear and

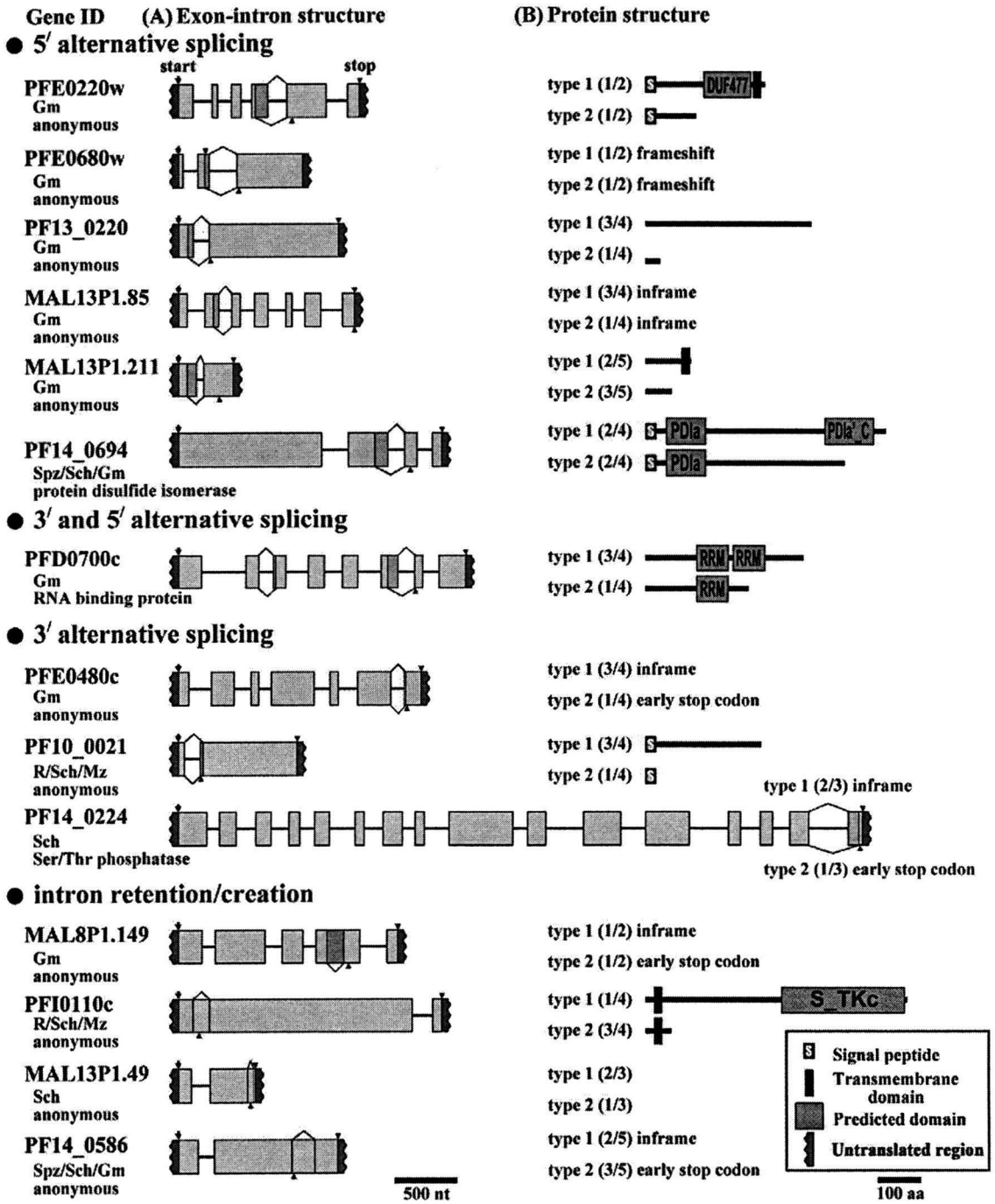

Fig. 1. Alternative splicing events that were detected in this study for *Plasmodium falciparum*. (A) Exon–intron boundaries for 2 types of transcripts are shown. Arrows indicate probable start codons. Arrowheads at the top or the bottom of each schematic indicate probable stop codons according to the exon–intron boundaries. Stage that transcribes each gene is shown under the Gene ID according to the transcriptome analysis [14]; Gm, gametocyte; Sch, schizont; R, ring; Mz, merozoite; Spz, sporozoite. Protein annotations refer to PlasmoDB [15]. (B) Predicted domain architectures of the proteins encoded by two variant transcripts. Type 1 is the presumed original transcript that encodes a longer open reading frame, whereas type 2 encodes a truncated product. The number of the clones for each type, per total clones, is shown in parentheses. Signal peptides and transmembrane domains were predicted by the SignalP and TMHMM2 programs, respectively. Domains were predicted by the SMART program (http://smart.embl-heidelberg.de/) or by searching the Conserved Domain Database (CDD) with Reverse Position Specific BLAST. Domains include: unknown function 477 (DUF477); thioredoxin domain of protein disulfide isomerase family (PDIa); C-terminal thioredoxin domain PDIa′ subfamily (PDIa′_C); Ser/Thr protein kinase motif (S_TKc); and the RNA recognition motif (RRM). The type of alternative splicing for the MAL8P1.149 is likely intron creation rather than intron retention, because type 1 possesses another intron and encoding longer open reading frame.

cytoplasmic activities of SR proteins was shown in mammalian cells [25]. A putative *P. falciparum* ortholog of SF2/ASF (PFE0865c and PF11_0205) might affect alternative splicing in *Plasmodium*. Interestingly, most of the *P. falciparum* genes reported to show alternative splicing are transcribed at the gametocyte and/or sporozoite stages [16], and this observation does not contradict our proposal.

In summary, among 88 isolated genes we found 14 genes that showed alternative splicing patterns, and half of these resulted in an alteration of the protein domain architecture. Splicing machinery initially recognized introns in *P. falciparum*, as suggested by the presence of intron retention, similar to the other unicellular eukaryote yeast. In addition, the pattern of alternative 5′ splicing, in combination with previous reports of the exon skipping, suggests that the exon is also recognized to initiate splicing in *P. falciparum*. This is an important observation, because unicellular eukaryotes are proposed to possess only an "intron definition" system, based on the data from yeast.

Acknowledgements

We thank T. Templeton for critical reading of the manuscript. Gametocyte rich cultures of *Plasmodium falciparum* were a kind gift from C. Long. This work was supported in part by Grants-in-Aid for Scientific Research 18390129 and 19406009 (to T. T.); Scientific Research on Priority Areas 19041053 (to T. T.) from the Ministry of Education, Culture, Sports, Science, and Technology, Japan; and, in part, by a Grant-in-Aid of the Ministry of Health, Labour, and Welfare (H20-Sinkou-ippan-013), Japan (to T. T.).

Appendix A. Supplementary data

Supplementary data associated with this article can be found, in the online version, at doi:10.1016/j.parint.2009.02.002.

References

[1] Markell EK, John DT, Krotoski WA. Medical parasitology. 8th ed. Philadelphia: WB Saunders; 1998.
[2] Wood V, Gwilliam R, Rajandream MA, Lyne M, Lyne R, Stewart A, et al. The genome sequence of *Schizosaccharomyces pombe*. Nature 2002;415:871–80.
[3] Gardner MJ, Hall N, Fung E, White O, Berriman M, Hyman RW, et al. Genome sequence of the human malaria parasite *Plasmodium falciparum*. Nature 2002;419:498–511.
[4] Ast G. How did alternative splicing evolve? Nat Rev Genet 2004;5:773–82.
[5] Stamm S, Ben-Ari S, Rafalska I, Tang Y, Zhang Z, Toiber D, et al. Function of alternative splicing. Gene 2005;344:1–20.
[6] Muhia DK, Swales CA, Eckstein-Ludwig U, Saran S, Polley SD, Kelly JM, et al. Multiple splice variants encode a novel adenylyl cyclase of possible plastid origin expressed in the sexual stage of the malaria parasite *Plasmodium falciparum*. J Biol Chem 2003;278:22014–22.
[7] Singh N, Preiser P, Rénia L, Balu B, Barnwell J, Blair P, et al. Conservation and developmental control of alternative splicing in *maebl* among malaria parasites. J Mol Biol 2004;343:589–99.
[8] van Dooren GG, Su V, D MC, Ombrain, McFadden GI. Processing of an apicoplast leader sequence in *Plasmodium falciparum* and the identification of a putative leader cleavage enzyme. J Biol Chem 2002;277:23612–9.
[9] Knapp B, Nau U, Hundt E, Kupper HA. Demonstration of alternative splicing of a pre-mRNA expressed in the blood stage form of *Plasmodium falciparum*. J Biol Chem 1991;266:7148–54.
[10] Bracchi-Ricard V, Barik S, Delvecchio C, Doerig C, Chakrabarti R, Chakrabarti D. PfPK6, a novel cyclin-dependent kinase/mitogen-activated protein kinase-related protein kinase from *Plasmodium falciparum*. Biochem J 2000;347:255–63.
[11] Volkman SK, Barry AE, Lyons EJ, Nielsen KM, Thomas SM, Choi M, et al. Recent origin of *Plasmodium falciparum* from a single progenitor. Science 2001;293:482–4.
[12] Tsuboi T, Takeo S, Iriko H, Jin L, Tsuchimochi M, Matsuda S, et al. Wheat germ cell-free system-based production of malaria proteins for discovery of novel vaccine candidates. Infect Immun 2008;76:1702–8.
[13] Trager W, Jensen JB. Human malaria parasites in continuous culture. Science 1976;193:673–5.
[14] Le Roch KG, Zhou Y, Blair PL, Grainger M, Moch JK, Haynes JD, et al. Discovery of gene function by expression profiling of the malaria parasite life cycle. Science 2003;301:1503–8.
[15] Bahl A, Brunk B, Crabtree J, Fraunholz MJ, Gajria B, Grant GR, et al. PlasmoDB: the *Plasmodium* genome resource. A database integrating experimental and computational data. Nucleic Acids Res 2003;31:212–5.
[16] Vinkenoog R, Veldhuisen B, Sperança MA, del Portillo HA, Janse C, Waters AP. Comparison of introns in a cdc2-homologous gene within a number of *Plasmodium* species. Mol Biochem Parasitol 1995;71:233–41.
[17] Romfo CM, Alvarez CJ, van Heeckeren WJ, Webb CJ, Wise JA. Evidence for splice site pairing via intron definition in *Schizosaccharomyces pombe*. Mol Cell Biol 2000;20:7955–70.
[18] Berget SM. Exon recognition in vertebrate splicing. J Biol Chem 1995;270:2411–4.
[19] Talerico M, Berget SM. Intron definition in splicing of small *Drosophila* introns. Mol Cell Biol 1994;14:3434–45.
[20] Shen J, Zu K, Cass CL, Beyer AL, Hirsh J. Exon skipping by overexpression of a *Drosophila* heterogeneous nuclear ribonucleoprotein in vivo. Proc Natl Acad Sci USA 1995;92: 1822–5.
[21] Mair GR, Braks JA, Garver LS, Wiegant JC, Hall N, Dirks RW, et al. Regulation of sexual development of *Plasmodium* by translational repression. Science 2006;313:667–9.
[22] Jumaa H, Nielsen PJ. The splicing factor SRp20 modifies splicing of its own mRNA and ASF/SF2 antagonizes this regulation. EMBO J 1997;16:5077–85.
[23] Gallego ME, Gattoni R, Stevenin J, Marie J, Expert-Bezancon A. The SR splicing factors ASF/SF2 and SC35 have antagonistic effects on intronic enhancer-dependent splicing of the beta-tropomyosin alternative exon 6A. EMBO J 1997;16:1772–84.
[24] Sanford JR, Gray NK, Beckmann K, Caceres JF. A novel role for shuttling SR proteins in mRNA translation. Genes Dev 2004;18:755–68.
[25] Blaustein M, Pelisch F, Tanos T, Muñoz MJ, Wengier D, Quadrana L, et al. Concerted regulation of nuclear and cytoplasmic activities of SR proteins by AKT. Nat Struct Mol Biol 2005;12:1037–44.

Single amino acid substitution in *Plasmodium yoelii* erythrocyte ligand determines its localization and controls parasite virulence

Hitoshi Otsuki[a], Osamu Kaneko[a,b,1], Amporn Thongkukiatkul[a,c], Mayumi Tachibana[a], Hideyuki Iriko[a,d], Satoru Takeo[e], Takafumi Tsuboi[e], and Motomi Torii[a]

[a]Department of Molecular Parasitology, Ehime University Graduate School of Medicine, Toon, Ehime 791-0295, Japan; [b]Department of Protozoology, Institute of Tropical Medicine (NEKKEN) and the Global Center of Excellence Program, Nagasaki University, Nagasaki, Nagasaki 852-8523, Japan; [c]Department of Biology, Burapha University, Amphur Muang, Chonburi 20131, Thailand; [d]Department of Microbiology and Pathology, Faculty of Medicine, Tottori University, Yonago, Tottori 683-8503, Japan; and [e]Cell-Free Science and Technology Research Center, Ehime University, Matsuyama, Ehime 790-8577, Japan

Edited by Thomas E. Wellems, National Institutes of Health, Bethesda, MD, and approved February 23, 2009 (received for review November 10, 2008)

The major virulence determinant of the rodent malaria parasite, *Plasmodium yoelii*, has remained unresolved since the discovery of the lethal line in the 1970s. Because virulence in this parasite correlates with the ability to invade different types of erythrocytes, we evaluated the potential role of the parasite erythrocyte binding ligand, *Py*EBL. We found 1 amino acid substitution in a domain responsible for intracellular trafficking between the lethal and nonlethal parasite lines and, furthermore, that the intracellular localization of *Py*EBL was distinct between these lines. Genetic modification showed that this substitution was responsible not only for *Py*EBL localization but also the erythrocyte-type invasion preference of the parasite and subsequently its virulence in mice. This previously unrecognized mechanism for altering an invasion phenotype indicates that subtle alterations of a malaria parasite ligand can dramatically affect host–pathogen interactions and malaria virulence.

dense granule | invasion | malaria | microneme | transfection

The rodent malaria parasite *Plasmodium yoelii yoelii* has been widely studied to understand the interactions between the malaria parasite and the host cell (1). The nonlethal 17X line mainly infects young erythrocytes (reticulocytes), whereas the lethal 17XL and YM lines infect a wide range of erythrocytes. These lines have previously been studied to identify the genetic determinants of virulence (2, 3). These differences in erythrocyte invasion preference suggest the possible involvement of a parasite ligand that recognizes erythrocyte surface receptors; however, the actual molecular basis of the observed invasion preference differences remains unclear.

Erythrocyte invasion by the malaria merozoite is a multistep process, initiated by reversible binding to the erythrocyte surface, followed by the establishment of a tight junction between the apical end of the merozoite and erythrocyte surface and the subsequent movement of the merozoite into the nascent parasitophorous vacuole. Each step involves specific interactions between parasite ligands and erythrocyte receptors. Among the ligands of malaria parasites, the best characterized is a type I integral transmembrane protein encoded by the *ebl* (*erythrocyte-binding-like*) gene family. Upon release from the micronemes, EBL proteins recognize erythrocyte receptors and initiate the formation of the tight junction. The importance of EBL in malaria virulence is exemplified in the human malaria parasite *Plasmodium vivax*, which uses an EBL orthologue, *Pv*DBP, to recognize the Duffy antigen on the erythrocyte surface. Because the parasite is apparently unable to use an alternative invasion pathway, individuals in whom the Duffy antigen is not expressed on the erythrocyte surface are completely resistant to *P. vivax* (4, 5). Because of this dramatic association between the disruption of a host–pathogen interaction and protection against a malaria parasite, *Pv*DBP and the *Plasmodium falciparum* EBL orthologue, EBA-175, have been targeted for vaccine development (6).

EBL proteins possess 2 Cys-rich regions conserved among EBL orthologues. The N-terminal Cys-rich region named the DBL (Duffy-binding-like) domain or region 2 (7) recognizes a specific erythrocyte surface receptor. The C-terminal Cys-rich region named the C-cys domain or region 6 is located adjacent to the transmembrane domain, and the number and location of Cys residues are well conserved among known *Plasmodium* species. Region 6 exhibits structural similarity to the KIX-binding domain of the coactivator CREB-binding protein (8) and has been proposed to be a protein trafficking signal for transportation to the micronemes (9). Here we report a single nonsynonymous nucleotide substitution in the *pyebl* gene between lethal and nonlethal lines of *P. yoelii* and show the effect of this substitution on the intracellular localization of EBL, erythrocyte-type preference, and consequently virulence of *P. yoelii*.

Results

To investigate differences in EBL between lethal and nonlethal *P. yoelii* lines, we compared sequences from a variety of malaria parasite species and *P. yoelii* lines 17X, 17XL, and YM. We found 1 nonsynonymous nucleotide substitution in region 6 between the nonlethal 17X and lethal 17XL lines in the entire ORF (Fig. 1). The nonlethal 17X line possesses 8 conserved Cys residues that form 4 disulfide bridges (8), whereas the lethal 17XL line possesses an Arg instead of Cys at the second Cys position. This substitution was also found in another lethal line, "YM" (2), which originated independently from the 17X line during serial passage (3). All *Plasmodium* EBL orthologues for which protein expression was validated possess 8 conserved Cys residues in this region, further indicating that these Cys residues play an important role (supporting information Fig. S1). Thus the observed substitution from Cys to Arg is likely to abolish the native conformation of region 6.

EBL Localizes in the Dense Granules in *P. yoelii* Line 17XL. We raised specific polyclonal and monoclonal antibodies against *Py*EBL

Author contributions: H.O., O.K., and M. Torii designed research; H.O., A.T., M. Tachibana, H.I., and S.T. performed research; T.T. contributed new reagents/analytic tools; H.O., O.K., and M. Torii analyzed data; and H.O. and O.K. wrote the paper.

The authors declare no conflict of interest.

This article is a PNAS Direct Submission.

Data deposition: The data reported in this article have been deposited in the GenBank/European Molecular Biology Laboratory/DNA Data Base in Japan databases (accession nos. AB430781–AB430789).

[1]To whom correspondence should be addressed. E-mail: okaneko@nagasaki-u.ac.jp.

This article contains supporting information online at www.pnas.org/cgi/content/full/0811313106/DCSupplemental.

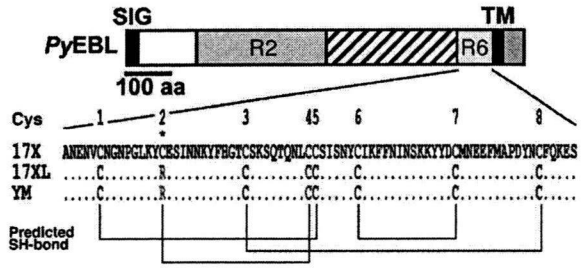

Fig. 1. Schematic structure of *P. yoelii* EBL (*Py*EBL). SIG, TM, R2, and R6 indicate the putative endoplasmic reticulum transporting signal, the transmembrane region, region 2, and region 6, respectively. Amino acid alignment of *Py*EBL from 17X, 17XL, and YM lines are shown below. Eight conserved Cys residues that form disulfide bridges (Predicted SH-bond) and the substitution from Cys to Arg (*) are indicated.

and performed Western blot analysis. The *Py*EBL protein was detected as a 110-kDa band in both the 17X and 17XL lines (Fig. 2*A*). The intracellular localization of *Py*EBL in both the 17X and 17XL lines was compared by indirect immunofluorescent assay

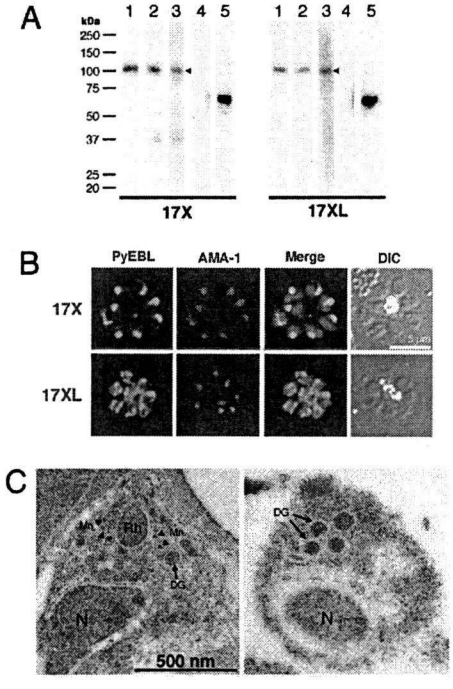

Fig. 2. Western blot analysis and *Py*EBL localization in *P. yoelii* schizont by immunostaining. (*A*) Western blot analysis with mAb 5B10 (lane 1), mAb 1G10 (lanes 2), and mouse serum (lane 3) specific for *Py*EBL against purified *P. yoelii* schizont extracts. A 110-kDa band was detected in both 17X and 17XL lines, with no significant difference in the protein expression level (arrowheads). This band was not detected by normal mouse serum (lane 4). Anti-AMA1 serum detected a 66-kDa band at similar levels (lane 5). (*B*) *P. yoelii* schizonts were incubated with mAb 5B10 (PyEBL), rabbit anti-AMA1 serum (AMA1), and DAPI (blue) for nuclear staining. Schizonts labeled with anti-*Py*EBL (5B10) were stained with FITC secondary antibody (green). Anti-AMA1 were stained with Alexa-546 secondary antibody (red). DIC images are shown in the right-hand column. The 17X line shows apical *Py*EBL signal colocalized with AMA1, but the region 6–substituted 17XL line shows diffused staining that does not colocalize with AMA1. (*C*) Immunoelectron microcopy was carried out for resin-embedded *P. yoelii* 17X and 17XL lines with anti-*Py*EBL mouse serum and secondary antibody conjugated with gold particles. *Py*EBL was detected in the micronemes (arrowheads) of the 17X line, but in the 17XL line it was located in the dense granules (arrows). N, nucleus; Mn, microneme; DG, dense granule; Rh, rhoptry.

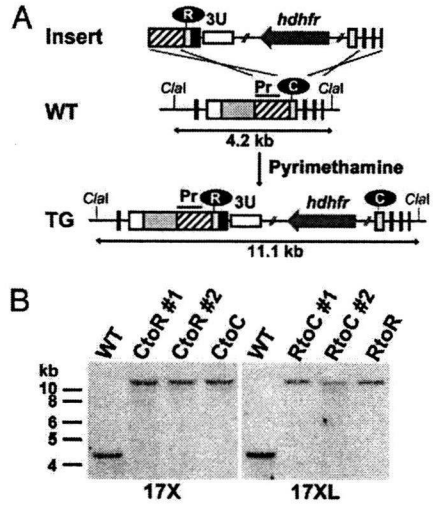

Fig. 3. Amino acid replacement of *Py*EBL region 6 second cysteine location by targeted recombination. (*A*) Schematic representation of the WT and modified (TG) *pyebl* gene loci. The replacement cassette (Insert) was inserted into the *pyebl* gene locus by double-crossover recombination. In this schematic, the second Cys in region 6 was replaced with Arg in the 17X line to generate 17X-CtoR. Other transgenic lines were generated in a similar fashion. ClaI restriction sites and the expected size of the DNA fragment after ClaI digestion are shown. Pr, probe region used in Southern blot analysis. (*B*) Southern blot analysis of the *pyebl* gene locus in WT and transgenic parasite lines derived from *P. yoelii* 17X and 17XL. The absence of the 4.2-kb WT band and the presence of an 11.1-kb band indicate that the *Py*EBL locus was modified in all transgenic clones.

(IFA) using specific antibodies against *Py*EBL (Fig. S2). In the 17X line, *Py*EBL localized to the apical end of each merozoite in both the segmented schizont-stage parasite and individual merozoites, where it colocalized with AMA1, a known microneme protein, under immunofluorescent microscopy (Fig. 2*B*). However, in the 17XL line *Py*EBL did not colocalize with AMA1 at the apical end of merozoites and showed a more diffused but granular distribution in comparison with parasites of the 17X line (Fig. 2*B*). Diffused localization of *Py*EBL was also observed in parasites of the YM line (Fig. S3). Immunoelectron microscopy revealed that *Py*EBL localized in micronemes in the 17X line as reported for *P. falciparum* and *Plasmodium knowlesi* (10, 11). In the 17XL line, however, *Py*EBL localized not in the microneme but in another microorganelle—the dense granules (12) (Fig. 2*C* and Fig. S4).

Because there seems to be only 1 copy of *Py*EBL in the genomes of both lines (Fig. S5), and significant differences were not observed in the level of transcription and protein expression between the 17X and 17XL lines (Fig. 2*A* and Fig. S6), the location of EBL seems to be the most significant difference between them.

Genetic Replacement of Arg and Cys in Region 6 Alters EBL Localization. To evaluate whether the Arg substitution at the second Cys position is responsible for the altered trafficking of *Py*EBL, we exchanged Cys and Arg in the 17X and 17XL lines by genetic modification (17X-CtoR and 17XL-RtoC). The parasites were also transfected with control constructs that do not alter the region 6 amino acid sequence (17X-CtoC and 17XL-RtoR) (Fig. 3*A*). Each of the transgenic parasites was evaluated for the correct integration of the constructs to the *pyebl* gene locus by specific PCR analysis followed by sequencing of the PCR-amplified products (not shown) and Southern blot analysis (Fig. 3*B*).

In the 17X line, replacement of Cys with Arg (17X-CtoR) altered the *Py*EBL localization from an apical pattern to a